Russian Chemical Reviews **68** (2) 103 – 118 (1999) © 1999 Russian Academy of Sciences and Turpion Ltd

UDC 541.16

Simulation of nanotubular forms of matter

A L Ivanovskii

Contents

I.	Introduction	103
II.	Theoretical models of electronic properties of ideal carbon nanotubulenes	104
III.	Defect structure of carbon nanotubulenes. Nanotubular composites	106
IV.	Electronic properties of several non-metal compounds in the nanotubular form	109
V.	Theoretical models of the growth and morphology of nanotubes	112
VI.	Nanotube crystals	114
VII.	Conclusion	116

Abstract. Data on the electronic and chemical structure of a new quasi-one-dimensional form of matter, *viz*., nanotubulenes, are generalised and systematised. Methods and approaches used in modern quantum chemistry for the simulation of the composition, structure, and properties of isolated tubulenes based on layered phases (graphite, boron nitride, boron carbide and boron carbonitride), nanotubular composites and nanotube crystals are described. The role of quantum theory in the development of the concepts of fundamental properties of substances in the nanotubular form and methods of their targeted modification is discussed. Prognostic potentials of theoretical models in solving material science problems are considered. The bibliography includes 197 references.

I. Introduction

The study of nanomaterials (NM) is one of the leading areas of investigation in modern chemistry. Nanomaterials that are currently produced in the form of isolated clusters, powders, films, and consolidated systems with a characteristic size of crystallites not more than 100 nm possess many unusual properties that are promising for the development of high technologies.[1–8] In addition, they form a unique class of objects used for studying fundamental problems of the metastable state of matter and the prospects of producing its new forms that have no analogues in nature.[2,6,8]

The greatest progress in this area has been achieved in the field of synthesis and comprehensive studies of a new allotropic modification of carbon, fullerenes, and first of all, 'classical' spheroidal carbon clusters (C_{60} and C_{70}), endohedral complexes, as well as film and crystalline materials based on these substances (fullerites).[1,2,8]

The topology and physicochemical properties of nonspherical carbon clusters built of a large number of atoms (the so-called giant fullerenes C_n, $n > 70$) have become the subject of numerous recent studies in which different types of closed carbon structures (capsulenes, torrenes, barrellenes, *etc*.) were discussed.[1,2]

Iijima[9] has discovered quasi-one-dimensional (quasi-1*D*) hollow tubular carbon fibres, *viz*., nanoscale carbon tubes (nanotubulenes), which are extended cylinders whose walls are formed by rolled graphite sheets. Carbon nanotubes with diameters ranging from five to several tens of nanometres and consisting of 2 to 50 coaxial graphite cylinders [the so-called multilayered nanotubes (MNT)] were detected[9] by transmission electron microscopy (TEM) in the soot obtained in arc-discharge experiments using graphite electrodes. More recently, both multilayered and single-layered nanotubes (SNT) were obtained.[10–16]

It was suggested[8,10] to consider nanoscale tubular structures as a new, quasi-1*D* form of carbon that occupies a 'vacant' position in the series of the known forms of carbon of different topological dimension 3*D* (diamond), 2*D* (graphite), and 0*D* (fullerene).

Almost simultaneously with the first reports on the syntheses of carbon NT,[10–16] several studies devoted to simulation of their electronic structure were carried out,[17–24] and unexpected and extremely interesting results were obtained. It was established that, depending on the NT diameter and the type of helical ordering of carbon atoms constituting the cylinder walls, tubulenes can possess both metallic and semiconducting properties.

The predicted possibilities of targeted modification of carbon NT conductivity have at once become the subject of daring hypotheses for their use in diverse exotic devices and elements of electronic circuits of uniquely small sizes (nanocoils, nanowires, *etc*.).[10,16] The list of possible 'nanoscale devices' in which electronic, optical, catalytic, capillary, and other properties of NT can be used, is increasing rapidly.[25–31]

In the first stage of experimental studies, methods of production of carbon NT and a number of nanotubular composites were developed. The results of there studies were generalised in a monograph.[8]

Recently, stable nanotubular structures based on several layered compounds, *viz*., BN,[32–36] BC_3,[37] BC_2N,[37,38] and MoS_2[39,40] have been synthesised and it was suggested that nanotubular forms of silicon[41,42] and boron[43] as well as consolidated nanotubular materials[44,45] can be obtained.

Research in the field of the synthesis and study of the properties of nanotubular forms of substances is intimately associated with the development of quantum chemistry of tubulenes, which is caused by several reasons. The interest of investigators in quasi-1*D* carbon NT and initiation of large-scale projects in the field of

A L Ivanovskii Institute of Solid State Chemistry, Ural Branch of the Russian Academy of Sciences, ul. Pervomaiskaya 91, 620219 Ekaterinburg, Russian Federation. Fax (7-343) 274 44 95. Tel. (7-343) 249 30 82

Received 21 April 1998
Uspekhi Khimii **68** (2) 119 – 135 (1999); translated by A M Raevsky

synthesis, physical chemistry, and material science of NT is to a great extent due to predicted unusual electronic properties of these objects.[17–24]

Nanotubulenes are obtained by vapour deposition in various media (see, *e.g.*, Refs 6, 8). For instance, carbon tubulenes are synthesised in arc-discharge apparatus in the presence of catalysts. As a rule, the final product is a mixture of NT and other carbon-containing species (*e.g.*, metal carbides), which hampers substantially the studies of the properties of NT themselves. Suffice it to say that the isolation of NT possessing semiconducting and metallic properties predicted in 1992 [17–24] was reported only recently.[46, 47]

Theoretical simulation of NT plays an extremely important role in the solution of the problem of obtaining the nanotubular substances 'in pure form': almost all the known substances in the nanotubular form and many of their properties were predicted from the results of calculations.

In the present review, the main stages of the development of ideas of the electronic properties of substances in the nanotubular form calculated first of all using modern quantum-chemical methods are considered. Particular attention is paid to the application of theory to the simulation of the structure and description of physicochemical properties of non-ideal nanotubulenes, nanotubular composites, and nanotubular crystals that are most interesting from the viewpoint of their practical use.

II. Theoretical models of electronic properties of ideal carbon nanotubulenes

The principles of theoretical description of ideal carbon single-layered NT were developed in 1992.[17–24] Schemes of NT classification were proposed and fundamental dependences between the atomic structure of cylindrical nanostructures and their electronic properties were established.

Saito *et al.*[18] considered the principles of the formation of two types of NT taking closed tubulenes as an example. Fullerene C_{60} hemispheres were taken as the end groups; they can be obtained as a result of dissecting the C_{60} framework in such a manner that the section plane contained 9 or 10 carbon atoms (Fig. 1). This respectively corresponds to the so-called 'arm-chair' or 'zigzag' cross sections. Since the type of ordering of the atoms constituting the cylinder walls closed by the above-mentioned end groups will be determined uniquely, the corresponding terminology is also used for the description of the NT obtained, and 'arm-chair' or 'zigzag' NT are considered (Fig. 2).

'Open' NT can also be constructed by rolling a planar atomic graphite sheet. In this case each cylinder is characterised by its diameter and the type of helical atomic ordering (chirality).[18, 19]

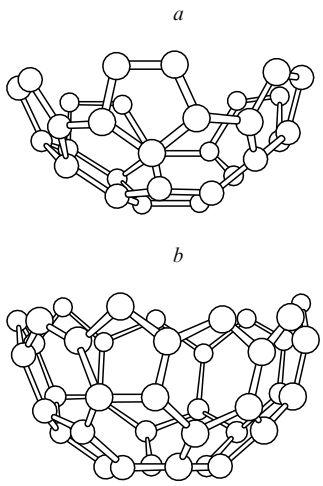


Figure 1. 'Arm-chair' (*a*) and 'zigzag' (*b*) cross sections of fullerene C_{60}.

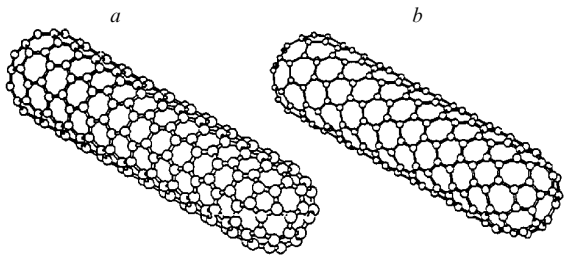


Figure 2. Structure of 'arm-chair' (*a*) and 'zigzag' (*b*) tubulenes.

Using the basis vectors of the graphite sheet $\mathbf{a}_1$ and $\mathbf{a}_2$ (Fig. 3), the diameter (d), and the pitch angle (θ), the vector

$$\mathbf{c}_n = n\mathbf{a}_1 + m\mathbf{a}_2$$

is given [the so-called (n, m)-NT]. The parameters d and θ are defined by the following relationships:

$$d = \frac{|c_n|}{\pi} = \frac{a\sqrt{3(n^2 + m^2 + mn)}}{\pi},$$

where a is the interatomic distance in the planar sheet, and

$$\theta = \arctan\left(-\frac{\sqrt{3}m}{2n + m}\right).$$

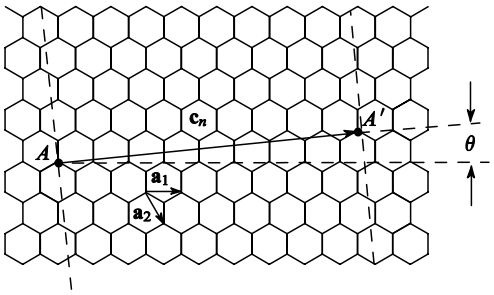


Figure 3. The method for selecting the vector $\mathbf{c}_n$ that defines the diameter and the pitch angle θ for an 'open' nanotube that can be constructed by rolling a graphite sheet (by matching the points A and A').

Depending on the indices n and m, chiral (n, m) and achiral (n, 0) nanotubes are distinguished.

Calculations of electronic properties for a large number of SNT with variable indices n and m were performed.[17–24] In Fig. 4, the distributions of the density of states (DOS) calculated by the tight-binding (TB) method for the (10, 0) and (9, 0) 'zigzag' carbon NT[19] are shown as an example. The energy bands are formed by mixed $\pi(2p_z)$ and $\sigma(2s,2p_{x,y})$ carbon states. Depending on the radius of curvature, carbon nanotubulenes can possess either metallic or semiconducting properties.

According to calculations,[17–24] there is a clear dependence between the structural indices (n, m) and conducting properties of ideal cylindrical single-layered tubulenes. All carbon (n, n)-NT possess a metallic type of conductivity. If $m \neq 0$ and $n = m + 3q$, where q is an integer, then the corresponding tubulenes are semiconductors with narrow band gaps, for which the band gap (ΔE_g) depends on the NT radius

$$\Delta E_g \simeq R^{-2}.$$

All other NT possess properties of semiconductors with wide band gaps, for which

$$\Delta E_g \simeq R^{-1}.$$

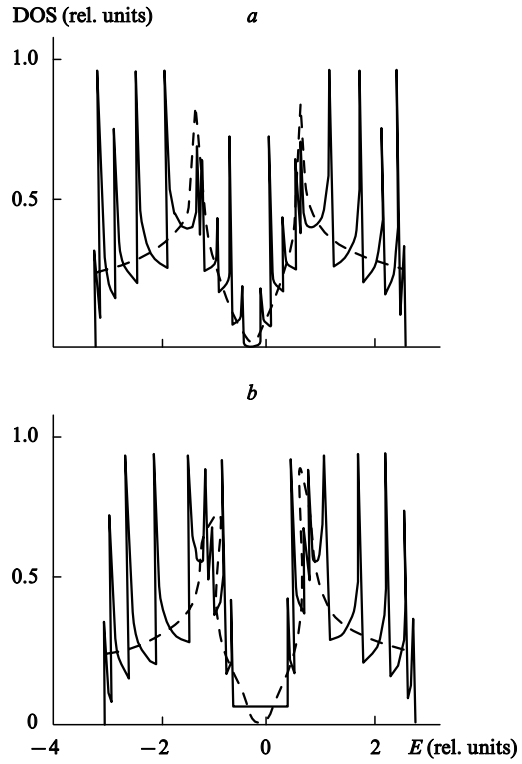


Figure 4. The total density of states (TDOS) for the 'zigzag' (10, 0)- (*a*) and (9, 0)-carbon nanotubulenes (*b*).[19] The TDOS for a planar graphite sheet is shown by dashed lines.
Calculations by the TB method.

It is natural that the relationships listed above are valid for the tubes of relatively small diameters, whereas at $d \to \infty$ the band structure of NT is transformed into that of a planar graphite sheet. This fundamental dependence of electronic properties of NT on their structure[17–24] was confirmed experimentally.[46,47] Two groups of NT with varied chirality were isolated and their current *vs*. voltage characteristics were measured. In accordance with theoretical predictions, a metallic or semiconducting type of conductivity was observed for these groups of NT depending on their structure.

Refinement of the details of electronic structure of carbon SNT was reported.[48–64] For instance, it was pointed out that $\sigma-\pi$-hybridisation should be taken into account in the case of semiconducting tubulenes of small radius.[50] A detailed study of this effect for NT with wide band gaps in the framework of the TB method made it possible to suggest an analytical dependence of ΔE_g on the tube radius.[34] The results of some calculations of (n, m)-NT with wide band gaps are listed in Table 1.

Table 1. Dependence of ΔE_g for carbon (n, m)-NT with wide band gaps on their radii.[26,54]

(n, m)	R /Å	ΔE_g /eV		
		see [a]	see [b]	see [c]
(7, 0)	2.7	0.79	1.11	1.00
(8, 0)	3.1	1.12	1.33	1.22
(10, 0)	3.9	0.65	0.87	0.85
(11, 0)	4.3	0.80	0.96	0.88

[a] Calculations[54] by the TB method in the parametrisation by Tomanek and Schluter.[59]
[b] Calculations[54] by the TB method in the parametrisation by Su *et al.*[65]
[c] Data taken from Ref. 26.

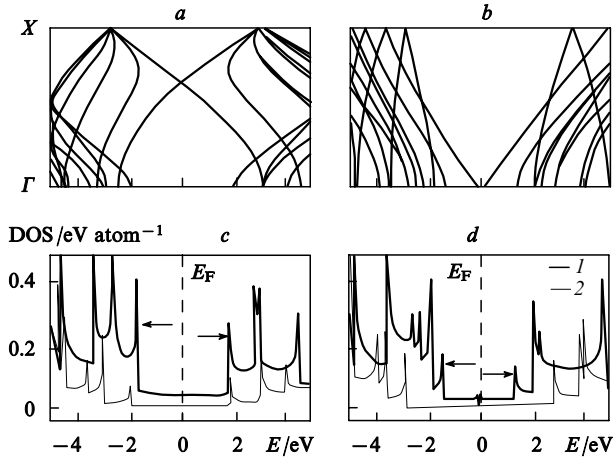


Figure 5. Dispersion of the energy bands (*a*, *b*) and the density of *p* (solid line) and *s* (dashed line) states of NT, (*c*) and (*d*), respectively; (*a*) and (*c*) (10, 5)-tubulene; (*b*) and (*d*) (9, 0)-tubulene. The δ-shaped DOS resonances near the Fermi level are shown by arrows.

The dependence of the DOS distributions on the NT radii and pitch angles was considered taking a group of metallic NT as an example.[50] The presence of a DOS 'plateau' near the Fermi level between the δ-shaped peaks (Fig. 5) separated by the E interval is a characteristic feature of carbon nanotubulenes with metallic (and quasi-metallic) types of conductivity [*e.g.*, the (10, 5) and (9, 0)-NT, respectively]. A general relation describing the $E(\theta, R)$ dependence was derived and numerical calculations of this spectral parameter were performed (Fig. 6). As can be seen, the E value (the width of the DOS 'plateau' near the Fermi level) is determined by the tube size, *viz*., E decreases substantially as R increases. For this reason, the parameters of the electronic states of tubulenes possessing metallic and semiconducting properties depend explicitly on their geometric indices.

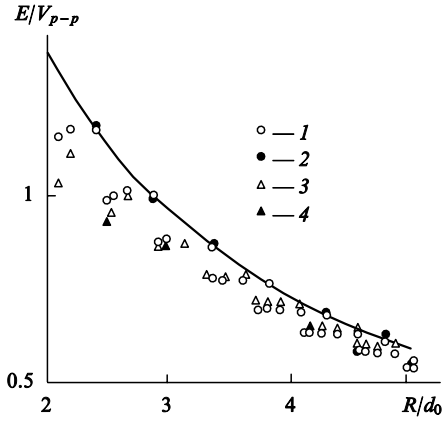


Figure 6. Dependence of the energy interval (E/V_{p-p}) between the δ-shaped DOS resonances near the Fermi level (see Fig. 5) for NT with metallic (*1*), (*2*) and quasi-metallic (*3*), (*4*) types of conductivity on their radii (R) referred to the C–C interatomic distance (d_0); V_{p-p} is the energy parameter used in TB calculations and determining the interaction between $p-p$ orbitals; (*1*), (*2*) $\theta = 30°$; (*3*), (*4*) $0 \leqslant \theta \leqslant 30°$.

The Peierls type of instability effects for metallic 1*D*-tubulenes was considered.[17–19] Based on the results of *ab initio* self-consistent calculations, it was shown[17] that, unlike, *e.g.*, *trans*-polyacetylene,[58] the temperature of the Peierls transition for the metal-like NT should be much higher than room temperature.[59]

The dependence of the stability of carbon tubulenes on their sizes was evaluated [60] and compared to similar data for other carbon nanoscale structures and macrostructures. The analysis was based on calculations of carbon atom binding energies (E_b) in NT. The calculations were carried out using two empirical potentials [61, 62] for a total of 169 nanotubes with $R < 9$ Å and pitch angles in the range $0^\circ < \theta < 30^\circ$ (the C–C distances were assumed to be equal to 1.44 Å). Several highly symmetric (n, n)-NT (n = 3, 4, 5, 6, 7, 9) were also calculated in the framework of the *ab initio* local electron density functional (LEDF) method.[63, 64] Figure 7 illustrates a clear dependence of the E_b of carbon atom on the NT geometric size ($E_b \sim R^{-2}$), according to which the binding energy of a carbon atom in NT approaches that of a carbon atom in graphite as the NT radius increases. As can also be seen, the E_b values of carbon atoms in fullerenes C_{60}, C_{180}, and C_{240} are higher than those of carbon atoms in the NT of corresponding radii. It was concluded that the formation of tubular or spheroidal nanoscale forms of carbon will be controlled not only by the energy state of a system, but also by the kinetics for the conditions of growth.

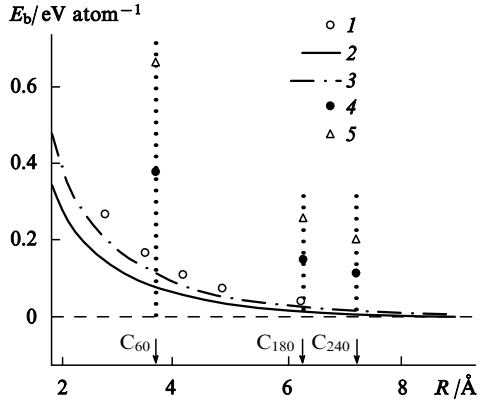


Figure 7. Binding energies of carbon atoms for nanotubes of various radii; (*1*) LDA calculations; (*2*) and (*3*) calculations by the pseudopotential method using data taken from Refs 27 and 28, respectively. The dashed line corresponds to the binding energy of carbon atoms in graphite. The binding energies of carbon atoms in fullerenes C_{60}, C_{180}, and C_{240} are also shown [the data were taken from Refs 27 (*4*) and 28 (*5*)].

The electron energy spectra (EES) of multilayered NT are much less studied than those of SNT. A double-layered NT (the radii of the 'outer' and 'inner' cylinders were 3.4 and 6.8 Å, respectively) was considered using the approximate density-functional computational scheme.[66] The calculations were carried out assuming a uniform surface electron density distribution without taking into account specific features of individual atomic geometry of the cylinders. It was found that the total density of states (TDOS) distribution for the double-layered NT was similar to that of SNT with characteristic oscillations reflecting the van Hove DOS singularities for 1*D* systems (Fig. 8). It is believed [66] that an increase in the number of layers will lead to the DOS of MNT approaching that of graphite.

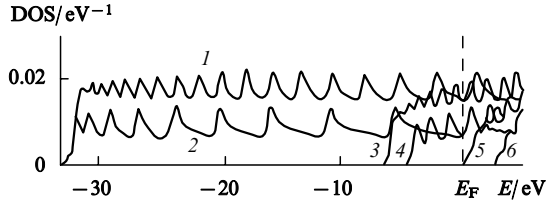


Figure 8. Decomposition of the TDOS for a double-layered NT into partial *s*- (*1*), (*2*), *p*- (*3*), (*4*), and *d*-components (*5*), (*6*) for the inner (*1*), (*3*), (*5*) and outer (*2*), (*4*), (*6*) nanotubes.[29]

On the whole, the results of quantum-chemical simulation of ideal cylindrical SNT made it possible to obtain a detailed description of their electronic properties and establish clear correlations between the parameters of the electron energy spectra, topology, and NT size. These results have become the basis for further calculations and predictions of some physicochemical properties of NT.

III. Defect structure of carbon nanotubulenes. Nanotubular composites

Investigation of defect NT is a certain stage of the development of the quantum chemistry of nanotubular forms of carbon. Both 'intrinsic' structural defects of tubulenes and various heterostructures involving NT (the so-called nanotubular composites) are considered.[6, 8] Three main types of 'intrinsic' defects of NT are distinguished, *viz.*, topological defects, rehybridisation defects, and defects of unsaturated (or 'dangling') bonds. In the first case, it is assumed that the rolled graphite sheet contains pentagons and heptagons (or their combinations). Rehybridisation defects are associated with the possibility of changing the standard sp^2 hybridisation of carbon atoms (*e.g.*, $sp^2 \rightleftarrows sp^3$). The third type of defects is due to vacancies, impurities, dislocations, and to the structure of the end groups (open or closed) of NT.

1. Structural defects and relaxation processes

The effects of quasi-1*D* structural relaxation capable of distorting the ideal cylindrical geometry of model NT were assessed [67] by the molecular-dynamics (MD) Car–Parrinello method [68] for a number of chiral and achiral NT. The 'optimised' structure of the (10, 0)- and (11, 5)-tubulenes considered [67] virtually coincides with the initial structure of the model rolled graphite sheet (the difference in the interatomic distances does not exceed ~ 0.01 Å). A possible explanation [67] is that the substance in the tubular form retains the main types of interatomic interactions characteristic of graphitic sheets.

Donor (nitrogen) or acceptor (boron) substitutional impurities [67] cause perturbations of the electron density and can affect the conducting properties of carbon NT. Local relaxation rearrangements upon N → C substitution are insignificant. When NT are doped with boron, the carbon atoms closest to the boron atoms are shifted along the bond axis by ~ 0.11 Å.

Charge distributions in the presence of substitutional impurities (individual B, N, and Si atoms, anions, and cations) were investigated [57] in the framework of embedded cyclic cluster model [69] by the MNDO/PM3 method taking a (6, 6)-NT as an example. It was pointed out that discrete donor or acceptor levels appear in the band gap of the tubulene. Defect-induced perturbations are propagated along the NT axis to a larger number of neighbouring spheres than those propagated along the circumference of the cylinder. Charged defects produce larger perturbation areas than neutral ones.

A topological type of defect associated with the formation of a carbon vacancy was considered.[70] Taking a metal-like (4, 4)-NT as an example, it was found that the number of conductivity channels (according to terminology [71, 72]) decreases in the presence of carbon vacancies, which leads to suppression of conducting properties of the NT.

2. Radial deformations of nanotubulenes

Charlier *et al.*[73] discussed the effect of change in the curvature of atomic layers along the circumference of the carbon cylinder on the electronic properties of NT. The possibility for non-cylindrical carbon NT with pronounced 'cut' of the walls to be formed was confirmed by three-dimensional holographic TEM images.[74–76]

It should be noted that the nature of microdeformations of carbon NT walls (the 'ripples' observed on the NT surface [77]) is associated with the rehybridisation effect, *i.e.*, with the change in

the effective hybridisation of the carbon atom from sp^2 to sp^3 (diamond). In this case, local protrusions of the surface that form 'structural waves' (folds) with variable curvature will be characterised by averaged $sp^{2+\alpha}$ carbon hybridisation, where the parameter α depends on the curvature of the microarea of the NT surface.

The edges of prismatic NT can be considered as visual lines of rehybridisation that occurs upon the change in the atomic configurations from sp^2 to sp^3, or as lines of hybridisation defects.[77]

Tight-binding DOS calculations for a cylindrical (10, 0)-tube and $(10, 0)^n$-tubes with n-gonal cross sections showed that in the latter case there is a number of peculiarities on the DOS profile such as clearly seen effects of $\sigma^*-\pi^*$ hybridisation and appreciable changes in the energy band structure. These peculiarities are characteristic of small-diameter NT.

In Fig. 9, the energy band structures of the (10, 0)- and $(10, 0)^5$-NT are shown as an example. The π^*-band energy of the $(10, 0)^5$-NT decreases substantially (the so-called NT 'metallisation'). The nature of this phenomenon becomes clear from comparing the charge density distributions (ρ) in the cross-sectional planes of cylindrical (10, 0)- and pentagonal $(10, 0)^5$-NT for the Γ-states near the Fermi level. The clearly seen ρ anisotropy at the vertices of the pentagon, partial outward shift of the charge density (the formation of σ-like states), and the reduction of the symmetry of the system lead to a substantial decrease in the band gap and to a change in the type of conductivity from semiconducting for the (10, 0)-NT to metallic for the $(10, 0)^5$-NT.

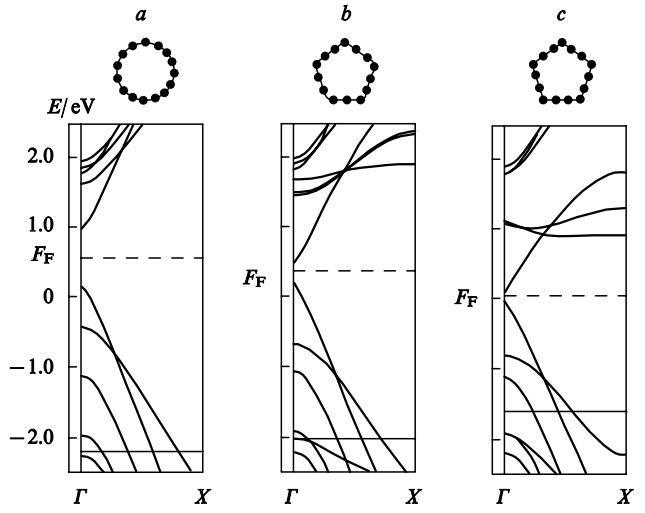


Figure 9. The energy band structures of (10, 0)- (*a*) and $(10, 0)^5$-NT (*c*), and a tubulene with 'intermediate' type of cross section (*b*).

Changes in the energy band structure of metal-like NT upon 'polygonisation' of their cross sections were considered taking $(12, 0)^n$-NT (n = 6, 4, 3) as examples.[73] It was established that the conducting properties of the NT change in the following order: metallic [(12, 0)-NT] → semiconducting $[(12, 0)^6$-NT with a band gap of about 0.5 eV] → metallic $[(12, 0)^4$- and $(12, 0)^3$-NT], which is mainly determined by the energies of the $\pi-\pi^*$ bands.

3. Uniaxial compression (tension) of nanotubes

Along with radial deformations in the cross-sectional plane, nanotubes can undergo longitudinal compressions (in particular, axial ones). This type of effect becomes of particular interest in connection with the investigation of mechanical properties of NT.[6, 8, 78, 79]

The effect of uniaxial stress on the density of states and type of conductivity of SNT was studied by the TB method taking 'zigzag' (n, 0) and 'arm-chair' (n, m) carbon nanotubulenes as examples.[80] A homogeneous uniaxial compression ($\sigma < 0$) and tension ($\sigma > 0$) was simulated by displacements of carbon atoms. Uniaxial stress will lead to the change in the NT chirality, which determines the energy characteristics of the cylindrical structures. It was found[80] that, depending on the index n and considering it as $(3q-1)$, $3q$, or $(3q+1)$, where q is an integer, the (n, 0)-NT can be arbitrarily classed into three groups. The band gaps of $(3q+1)$-NT will increase while those of $(3q-1)$-NT will decrease upon compression of (n, 0)-NT. The type of conductivity of the ($3q$, 0)-NT changes from metallic to a semiconducting one; for this reason, these NT are the most convenient objects for experimental testing of the dependence predicted.[80]

For all (n, 0)-NT considered,[80] the band gaps depend linearly on the modulus of compression (σ). According to the estimates[80] the band gap sensitivity to stress, $|dE_g/d\sigma|$, is about 10.7 meV GPa^{-1} in the range $|\sigma| < 10$ GPa. All metal-like 'arm-chair' (n, m)-NT retain their properties upon uniaxial stress.

The effect of compression on the electronic characteristics and other properties (in particular, on chiral currents) of nanotubulenes was studied by the self-consistent electron density functional method taking a group of carbon NT as an example (Table 2).[81] It was found that the major effect of compression of (9, 7)-NT consists in an appreciable increase in the band gap due to a decrease in the dispersity of π and π^* bands near the Fermi level. It is possible to make the system conducting by introducing hole or electron carriers. This can be done by doping NT with atoms of alkali metals (AM) or halogens. Miyamoto[81] simulated this effect by fixed shift of E_F. By solving the Boltzmann equation the components of the conductivity tensors of NT were found and the pitch angles for charge carrier currents were determined (see Table 2). It was stated[81] that violation of the symmetry of the hexagonal atomic ordering of the cylinder walls upon its compression can cause chiral currents to flow. This effect is most pronounced for the 'arm-chair' NT.

Table 2. Geometric parameters of compressed (n, m)-NT and pitch angles of chiral currents (θ') in the case of doping with electrons (e) and holes (h).

Geometric parameters of (n, m)-NT				θ'/deg (see [a])
(n, m)	d/Å	θ/deg	degree of compression (%)	
(13, 1)	10.78	4.1	10	1.6(h) 8.8(e)
(11.4)	10.60	15.5	10	0.5(h) 12.4(e)
(9, 7)	10.97	24.9	5	4.2(h)

[a] The calculations were carried out assuming that E_F is shifted by 50 meV from the bottom of the conduction band and from the top of the valence band upon doping of NT with electrons and holes, respectively.

TEM images[82–84] indicate that carbon NT can undergo diverse changes in their shapes and spatial configurations and that the types of NT deformations considered (radial and uniaxial) are a particular case of such changes. Studies of arbitrarily deformed NT are scarce due to the complexity of the description of their electronic properties.

4. Deformations of carbon nanotubulenes

As a rule, the problems of deformational behaviour of NT are studied in the context of the development of 'nanomechanics'. Most of experimental studies in this line[6, 8, 78, 79, 85–90] have been devoted to investigation of the brittle–elastic properties of NT under different conditions of external strain.

The microscopic simulation of the energy characteristics of mechanically deformed NT was performed by MD methods[88, 91]

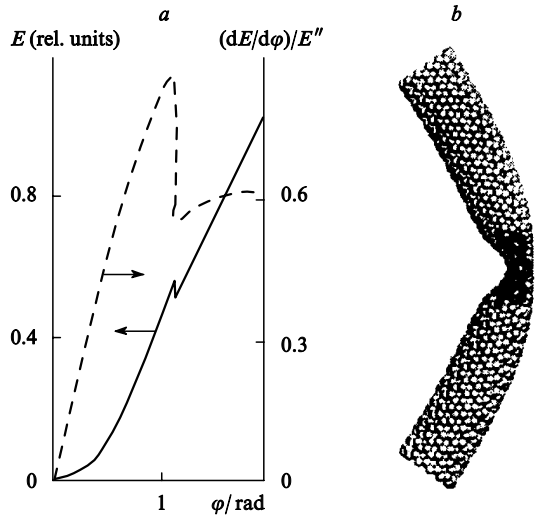


Figure 10. Dependence of the strain energy (E) and its derivative ($dE/d\varphi$) on the bending angle (φ) for the (13, 0)-NT (*a*) and the NT shape upon 'kink' (*b*).

using many-body interatomic potentials [61, 62] and energy parameters obtained in band structure calculations of 'slightly deformed' NT.[60, 92, 93]

Typical of this investigation line are MD calculations of the brittle–elastic properties of NT exposed to classical types of deformation (compression, bending, and torsion).[88, 91] Figure 10 illustrates the results obtained from MD calculations of the strain energy dependence of a (13, 0)-NT, 8 nm in length and 1 nm in diameter, on the tube bending angle. External strain was applied to both tube ends. The strain energy smoothly increased before the tube 'kink' (or inelastic bending) and sharply decreased afterwards.

The results of calculations [88, 91] reproduce the observed singularities on the strain–stress curves of NT of different dimensionality and are in good agreement with the experimental results.[8, 85–89] This makes it possible to point to the development of theoretical foundations of the nanomechanics of nanotubular objects.

Quantum-chemical calculations of electron states were carried out only for certain possible statistical configurations of deformed NT, *e.g.*, for uniform and non-uniform tubular helices (Fig. 11) [94] both predicted theoretically [95] and observed using the TEM technique.[96, 97] In addition to hexagons, the walls of helices include various heptagonpentagon combinations. Helical NT are an extensive class of objects related to toroidal carbon nanostructures.[8, 20, 98–102] The topology of helical NT is described [96, 103] using the Kekule structures and the concept of 'phason lines'.[104] Tight-binding calculations [94] showed that the energy band structure (in particular, the change in the band gap ΔE_g) depends strongly on the topology of the NT helices: an interrelation has been found between the arrangement of the 'phason lines' in the helices and the type of their conductivity.

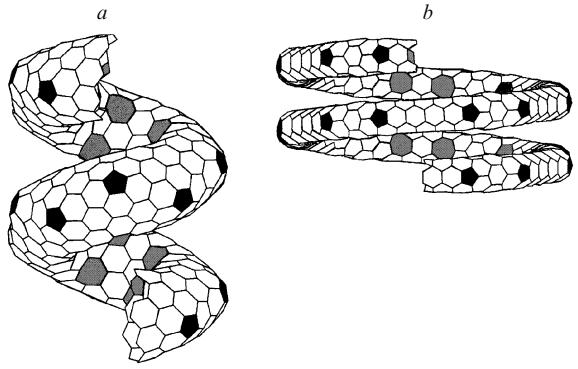


Figure 11. Models of helically deformed uniform (C_{360}) (*a*) and non-uniform (C_{540}) (*b*) tubular structures.[94]

5. Connection of nanotubulenes

Targeted introduction of topological defects into an NT, *i.e.*, replacement of a part of hexagons in the rolled graphite sheet that forms tubulene walls by other polygons (heptagons or pentagons) can change substantially its electronic properties. In this case, the theoretically predicted possibility of the formation of heterojunctions based on NT [6, 8] opens wide prospects for using carbon NT as the elements of integrated circuits of uniquely small size.

This situation can be considered from the viewpoint of longitudinal connection of two different tubulenes in which heptagons, pentagons, and their various combinations play a determining role in the formation of matched structures of NT (Fig. 12), thus opening new possibilities of producing electronic $n-p$ transitions.

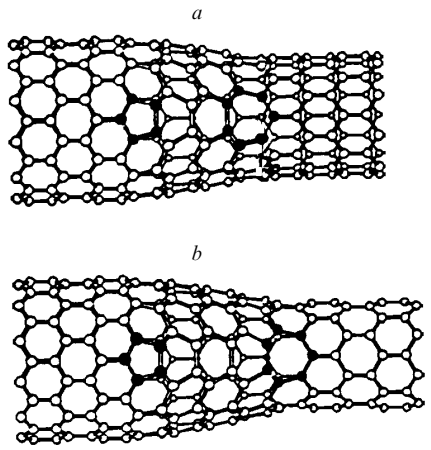


Figure 12. Variants of longitudinal connection of 'zigzag' carbon tubulenes; (*a*) (12, 0)/(9, 0)- and (*b*) (12, 0)/(8, 0)-tubulene. Carbon atoms participating in the formation of heptagons and pentagons in the structure of intertubular connectors are shown as bold solid circles.

It should be noted that the above-mentioned polygons (pentagons and heptagons) can be constituents of the ends of 'open' nanotubes and impart to them a conical shape of variable conicity, which can become of great importance for the development of nanoscale electron-emitting devices based on NT.[105]

Different types of matching and the properties of carbon NT of different diameter involving a heptagon–pentagon pair were simulated by the TB method taking (12, 0)/(9, 0)- and (12, 0)/(8, 0)-tubulenes as examples (see Fig. 12).[106] According to calculations performed taking into account only π-states, there are delocalised states for each of the tubulenes and localised states corresponding to open ends of NT ('dangling' bonds) in the spectrum of the entire system. The estimates [106] of the dependence of conducting properties on the voltage applied (U) showed that the current I increases as U increases for matched (12, 0)/(9, 0)-nanotubes with metallic type of conductivity and that oscillations corresponding to resonances of tunnelling probability between the two NT are observed on the current *vs.* voltage plot. The conductivity of the system of connected metallic (12, 0)- and semiconducting (8, 0)-nanotubes will be determined by the contribution from the (12, 0)-tubulene to the region near the Fermi level in the spectrum of the entire system.

A more detailed consideration of the EES of carbon NT with variable number of topological defects (pentagon–heptagon pairs, or 5/7-defects) of the wall surfaces of 'zigzag' (n, 0)-tubu-

lenes was carried out.[107] A system of (12, 0), (11, 0), and (9, 0)-nanotubulenes matched in pairs using one, two, and three pentagon – heptagon pairs arranged either along the cylindrical axis or along the cylinder circumference was calculated. The data listed in Table 3 illustrate the change in the energy of NT with topological defects (relative to that of 'perfect' tubulenes). As can be seen, in the general case, an axial arrangement of the 5/7-defect is the most energetically favourable. Even more energetically favourable is the formation of a specific type of defect in which a pentagon and a heptagon are separated by rings of hexagons (the 5/6/7-defect, see Table 3).

Table 3. Energy changes (relative to the energies of 'perfect' tubulenes) for different types of nanotube connection depending on the type of the arrangement of topological defects.

NT system	Number of defects	ΔE / eV atom^{-1}		
		5/7 defects along the circumference	axial 5/7 defects	specific defect [a]
(12, 0)/(11, 0)	one 5/7	0.132	–	–
(12, 0)/(11, 0)	two 5/7	0.258	0.249	0.208
(12, 0)/(9, 0)	three 5/7	0.405	0.291	–

[a] 5/6/7-Defect, see text.

Regularities of the rearrangement of electron states near the Fermi level in the region of hetero-junction can be traced taking a matched (12, 0)/(11, 0) metallic – semiconducting NT with optimised geometry as an example (Fig. 13). On going from the last segment of the (12, 0)-NT to the first segment of the connection structure, the DOS oscillations relative to the DOS 'plateau' of isolated (12, 0)-NT are observed near E_F. Similar DOS oscillations of gradually decreasing amplitude are observed when moving further along the connection structure toward the first segment of the (11, 0)-NT. The first segment of the (11, 0)-NT is gapless, which manifests itself as a smooth metal to semiconductor transition. The DOS of the hetero-junction structure approaches those of individual nanotubulenes at a distance of ± 20 Å from the connection structure on each side of the cylinders.

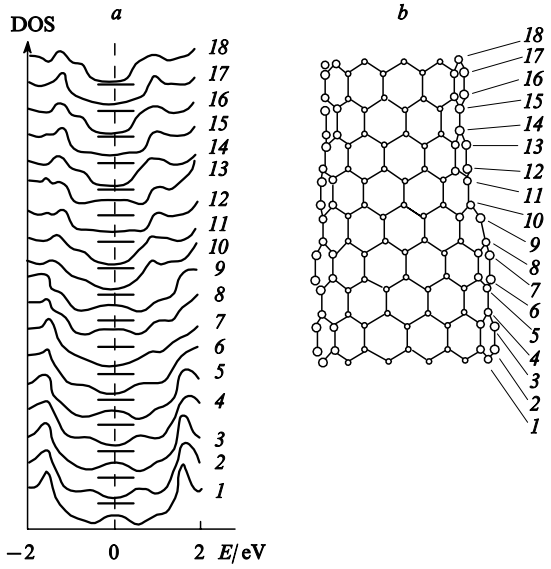


Figure 13. The electron density of π states (*a*) and the cross sections (*1*) – (*18*) of the intertubular connector structure for the (12, 0)/(11, 0)-NT (*b*).

6. Nanotubular composites: intercalation of carbon nanotubulenes

Intercalation of NT with atoms of various elements makes it possible to obtain quasi-1*D* nanomaterials with varied properties. For instance, it is possible to obtain composites by incorporating metal wires into NT. These can be used as nanowires of uniquely small cross section in which the tubulene simultaneously acts as both an insulator and a protective shell (*e.g.*, in oxidation processes). The properties of the components can change substantially upon interaction between the metal nanowire and NT (*e.g.*, new phases of a metal 'encapsulated' into the NT can be formed). This interaction can also cause a non-trivial modification of the properties of the entire hetero-system. For instance, its electron-phonon spectra and superconducting properties can be changed appreciably by intercalating the NT with alkali metals (AM), as is observed for fullerenes doped with AM or for intercalated graphite (see, *e.g.*, Ref. 8).

In most of experiments on NT intercalation, multilayered tubulenes of large diameter (> 100 Å) were obtained, which were filled (either directly in the synthesis or using the capillary effect) with Mg, Bi, Pb, several transition metals, lanthanides, and their carbides.[108 – 117]

These systems are considered in the framework of several computational schemes. Semiempirical MNDO calculations [57] of (n, 0)-tubulenes (n = 6, 8) with one or two encapsulated monatomic potassium wires oriented along the cylinder axis were performed using the embedded cyclic cluster model. It was found that the band gaps characteristic of initial NT disappear in the intercalated systems because of the appearance of new K 4*p* states. As a result, the K@(n, 0) systems are 1*D* conductors.

A quasi-1*D* hetero-structure consisting of a carbon nanotube (R = 3.4 Å) filled with a Pb nanowire (r = 2.4 Å) was considered.[66] Taking into account the approximations used in the calculations (a numerical method [118] was employed), Östling *et al.*[66] could only suggest that the electron states of the Pb nanowire will hybridise mainly with the near-the-Fermi-level π-states of the tubulene.

More rigorous calculations of (4, 4)-NT intercalated with 1*D* potassium and aluminum wires were carried out by the *ab initio* pseudopotential method.[119, 120] It was assumed that the metal wires and the (4, 4)-NT constitute commensurate 'phases' and that the interatomic distances in the wires are the same along the whole tube length. For the K@(n, n)-NT system, the energy effect of intercalation (heat of formation) was also calculated depending on the tubulene diameter ($\sim$ 1 eV atom^{-1} K^{-1}).[119] The corresponding value for the Al@(4, 4)-NT system was found to be negative[120] and it was assumed that intercalation of Al into the (4, 4)-NT can occur only in the gas phase under high pressure. Under normal conditions, only carbon nanotubes of large diameter can be intercalated with aluminum.

The results obtained [119, 120] show that quantum-chemical methods can be effectively used for solving important problems related to search for compositions of nanotubular composites and conditions of their production. Taking into account promising technological applications of these materials, one can expect the development of the material science of this class of substances.

IV. Electronic properties of several non-metal compounds in the nanotubular form

The progress in the synthesis and the study of the properties of carbon NT has initiated investigations on the search for tubular nanostructures of other substances. Hexagonal boron nitride (h-BN), an isoelectronic and isostructural graphite analogue, was proposed [121, 122] as the first candidate. It should be noted that the syntheses of the nanotubular form of BN and some other boron compounds [32 – 38] were performed on the basis of predictions made in the first theoretical studies on their structure and properties.[121 – 124]

Based on similarity in the structural and electronic properties of the known 2*D* boron compounds (h-BN, BC_3, and BC_2N [125, 126]) and graphite, the theoretical approaches successful in calculations on the tubular forms of carbon were used.[121–124]

1. Boron nitride-based nanotubulenes

Electronic properties of nanotubes based on h-BN were considered.[121, 122, 127] The dependence of the EES of chiral and achiral (*n*, *m*)-NT on their diameters was studied using a simple *s*,*p* TB model.[122] It was found that all the boron nitride nanotubulenes (BNT) considered are semiconductors in which the band gap (ΔE_g) decreases as the tube radius decreases. Chiral (*n*, *m*)-NT are less sensitive to variations of the tube radius than (*n*, 0)-NT. In addition, (*n*, 0)-NT are semiconductors with direct gaps ($\Gamma-\Gamma$), whereas (*n*, *m*)-NT have indirect band gaps ($\Delta-\Gamma$). Changes in ΔE_g upon varying pitch angles θ are most pronounced for the tubes of small diameter. Nanotubes with $d > 12$ Å have wide band gaps which depend slightly on θ. The following qualitative explanation can be proposed: in NT of small radii, the number of nonadjacent atoms is larger, and the distances between them appear to be comparable with interlayer separations in h-BN.

MNDO calculations of the electronic properties of (*n*, 0)- and (*n*, *n*)-BNT ($n = 6, 7, 10, 12$) were performed.[57] All NT were referred to dielectrics ($\Delta E_g \simeq 4.8$ eV). The position of the bottom of the conduction band is determined mainly by boron *s*, *p* states, whereas that of the top of the valence band is determined by nitrogen states.

More rigorous LDA calculations [121] of (*n*, 0)- and (*n*, *n*)-BNT with diameters in the range from 4.0 to 12.0 Å indicate that they are semiconductors with wide band gaps ($\Delta E_g \simeq 5.5$ eV). Because of this, the dependence of the electronic properties of BNT on their size and structure is less pronounced than in the case of graphite-based tubes. This fact is of importance for the preparation of nanomaterials with preset parameters.

When analysing the bands near the Fermi level, it was found that the states of the bottom of the conduction band are similar to those of 'quasi-free' electrons.[121] These states are concentrated in the inner part of the tube (Fig. 14). This peculiarity may have important technological applications in the doping of BNT with electron carriers, which would make it possible to vary their electrophysical properties over a wide range.

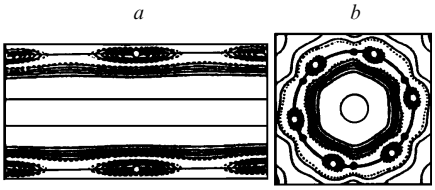


Figure 14. The total charge density distribution in the longitudinal section (including nitrogen atoms) (*a*) and in the cross section (*b*) of the (6, 6) BNT (LDA calculations).

Interesting results were obtained in the optimisation of the geometry of BNT.[121] It was shown that this tubular structure can be considered as a 'double-layered' structure consisting of oppositely charged coaxial cylinders that form a specific quasi-1*D* dipole. The boron ions constitute the 'outer' cylinder, while the nitrogen ions constitute the 'inner' one. The 'intercylinder' distance depends slightly on the tube chirality and decreases as its diameter increases. The total energy (E_{tot}) of BNT appeared to be lower than that of carbon NT of the corresponding diameter (Fig. 15). Comparison of the total energies of a BNT and an h-BN 'strip' obtained upon the 'development' of the corresponding cylinder showed that the 'strip' form of h-BN is much less stable than its tubular form.

It was established that if the distance between the tube walls in double-layered BNT [*e.g.*, a (4, 4)@(9, 9)-NT] is comparable with

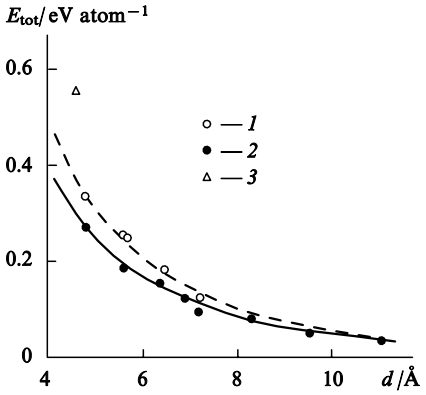


Figure 15. Dependence of the total energy (E_{tot}) on the diameter (*d*) for carbon (*1*) and BN (*2*) nanotubes. The E_{tot} value for a 'strip' obtained by 'developing' the (6, 0)-BN nanotube (the point *3*) is shown.

the interlayer separation in crystalline h-BN, the intertubular interaction has virtually no effect on the structure of electron states of individual NT. Single-layered and multilayered BN tubulenes are stable semiconductors with wide band gaps.[121]

Simulation of hetero-structures based on boron nitride tubulenes was first performed by Rubio *et al.*[128] who considered (4, 4)-BN-tubulenes intercalated with K and Al. It was assumed that, taking into account the peculiarities of the electronic structure of BNT,[121, 122] the interaction between the metal atoms and the NT walls will be appreciably weaker than for carbon tubulenes. The estimated intercalation energies (the difference between the total energies of the composite and its components, *viz.*, the tubulene and the metallic wire) of these hetero-structures appeared to be much lower than those of analogous systems based on carbon NT. The K 4*s* states of the K@(4, 4)-BNT were found to interact with the tubulene band near the Fermi level (Fig. 16). For an Al@(4, 4)-BNT, it was found that additional Al *s* and p_z levels

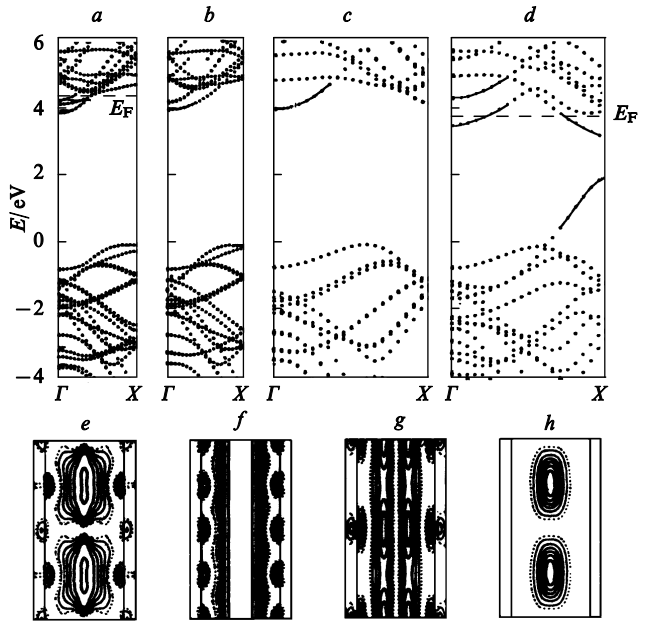


Figure 16. Energy band structures (*a*)–(*d*) and charge distributions (*e*)–(*h*) for the (4, 4)-BNT and for the composite K@(4, 4)-BNT and Al@(4, 4)-BNT.
The energy bands: (*a*) K@(4, 4)-BNT; (*b*) and (*c*) (4, 4)-BNT for single and double unit cells, respectively; and (*d*) Al@(4, 4)-BNT. Charge distributions for the states near the Fermi level are shown for longitudinal sections of the tubes. For the composite Al@(4, 4)-BNT, the contributions from Al *s* states are shown by solid lines.

appear in the band gap. The EES of the Al@(4, 4)-BNT appeared to be close to a simple superposition of the spectra of a monatomic Al wire and a (4, 4)-tubulene, which indicates a weak interaction between them. The plots of the charge density distributions for the near-the-Fermi level states in the K(Al)@(4, 4)-BNT (see Fig. 16) show that the density of electron carriers that control the conductivity of intercalated BNT is localised inside the cylinder. This differs these systems from composites based on carbon NT in which the contribution to the conductivity from the tubulene walls dominates. For this reason, BNT can be preferred (as compared to carbon tubulenes) for production of the nanowires with preset properties. The possibility of intercalation of BNT with Ag and Au atoms for production of continuous nanowires [127] cannot also be ruled out.

2. Boron carbide-based nanotubulenes

Electronic characteristics of some hypothetical $(n, 0)$-NT based on layered BC_3 were considered.[124] The conductivity type changes from metallic to semiconducting as the NT diameter increases. This effect is associated with noticeable deviations of the bond angles (for NT of small diameter) from 120°. With an increase in the NT diameter, the bond angles approach the ideal value for planar sheets (120°), and ΔE_g for NT approaches the band gap of single BC_3 sheets (see, *e.g.*, Refs 125 and 126). The analysis of the DOS distribution for a BC_3-tubulene shows that the lowest unfilled bands are composed of π- and π*-states and the highest filled bands are composed of σ-states. Near the Fermi level, the density of σ-states is considerably higher than that of π-states. It is assumed that the conductivity of a BC_3-NT of a fixed diameter can be varied over a wide range upon doping by varying the degree of filling of the energy bands. In this case, 'metallisation' of the σ-band, *i.e.*, a decrease in the concentration of electrons, will be a more efficient way of increasing the NT conductivity. Additional holes can appear upon partial replacement of carbon atoms by 'superstoichiometric' boron atoms. Atoms of halogens (Cl, Br, I) can also act as hole donors, as is the case for, *e.g.*, intercalated graphite-based compounds.[124]

Strain energies of BC_3 nanotubes were calculated.[124] The total energies of these tubulenes appeared to be lower than those of graphite-based NT. Further studies of BC_3-nanotubes should be carried out taking into account not only single-, but also multi-layered nanotubes, since it is known that the interlayer interaction plays a decisive role in the formation of conducting properties of crystalline BC_3.[125]

3. Boron carbonitride-based nanotubulenes

Depending on the ordering type of atoms (B, C, N) constituting the layers and on the type of layer-by-layer packing, graphite-like boron carbonitrides can possess either metallic or semiconducting properties.[125, 126] In addition, the strong 'intralayer' anisotropy of charge distributions suggests that circular chiral currents can arise upon rolling the single layers into cylinders. In this case the NT can be considered as nanoscale solenoids.

The geometry of several (n, n)-BC_2N nanotubes was calculated by the TB method.[123] Nanotubulenes of small diameters ($n = 2$) retain the conductivity type intrinsic in the initial BC_2N single layers.[125] However, for (n, m)-NT the change in the conductivity type from metallic to semiconducting is possible depending on their diameters and chirality (like for graphite-based NT). It is assumed that (n, n)-NT should be the most stable, since their atomic configuration provides the maximum number of the strongest C–C and B–N bonds.

According to Miyamoto *et al.*,[123] partial replacement of carbon atoms by 'extra' B or N atoms leads to the appearance of donor or acceptor impurity levels, respectively, in the band energy spectrum of carbonitride NT. This occurs due to the increase in the concentration of electrons or holes in $B_{1-x}C_{2+x}N$ or $BC_{2+x}N_{1-x}$ nanotubes, respectively. Calculations of chiral currents for doped BC_2N-tubulenes were carried out and the magnitude of induced magnetic field was evaluated.[129]

4. 'Mixed' boron carbonitride-based nanotubulenes

Hypothetical 'mixed' single-layered NT built of segments of carbon and BN hexagons that alternate either along the tube circumference or along the tube axis are considered as an example of possible quasi-1*D* systems possessing interesting quantum properties. They were studied by the MNDO method.[57] The following combinations of packing of carbon and BN hexagons were considered: alternation of C_6 and B_3N_3 'belts'† along the circumference of a (6, 6)-NT ($kB_3N_3 + lC_6$; $k = 3, 2, 1$; and $l = 1, 2, 3$, respectively) and alternation of strips† of hexagons along the tube axis ($kB_3N_3 + lC_6$; $k = 1, 2, 3, 4, 5$; and $l = 5, 4, 3, 2, 1$, respectively). We present here only the most important conclusions.[57] The introduction of a 'belt' or a strip of carbon hexagons substantially reduces ΔE_g of the boron nitride NT. An increase in the number of carbon fragments is accompanied by further decrease in the ΔE_g value. The introduction of 'belts' or strips of carbon hexagons between dielectric B_3N_3 'belts' or strips leads to the appearance of additional states in the band gap of the (6, 6)-BN tubulene, with the major contribution from the 'frontier' atoms of contacting different strips or 'belts'. For a 'belt' structure of mixed tubulenes, the contribution of carbon states to the bands near the Fermi level dominates, thus controlling the conducting and magnetic properties of the C_6 'belts'.

5. On the possible existence of nanotubular forms of boron

The results of calculations [43, 130–134] of elemental boron clusters have led to unexpected and non-trivial conclusions about possible directions of structural evolution of isolated boron microparticles upon their aggregation into larger associates.

Calculations [43, 130–134] were carried out using the Hartree–Fock methods with different basis sets (STO-3G, 3-21G, and SCF/DZ) and the local electron density functional method. The energy band structure was calculated for boron clusters with optimised geometry. A large number of topologically different B_n forms (starting from B_7) was designed. Three main possible types of their structural evolution were revealed, which lead to the formation of stable forms of boron clusters: (1) three-dimensional (3*D*) due to the growth of individual fragments of the structure of crystalline boron; (2) convex clusters (segments of a sphere or a cylinder); and (3) quasi-planar clusters.[126]

Nanotubes can also be formed in the bulk of α-boron quasi-crystals.[132, 133] This follows from calculations of possible local structural transformations in the bulk of an α-boron quasi-crystal with a 'compressed' rhombohedral unit cell for one of its fragments, *viz.*, joined B_{12} icosahedra, lying on the minor diagonal of the rhombohedron. The structure of the B_{24} group changes substantially in the course of optimisation. The stages of structural evolution of the B_{24} fragment are illustrated in Fig. 17. 'Diffusion' of the boron atoms located between the B_{12} icosahedra leads to the formation of a closed pseudotubular group (see

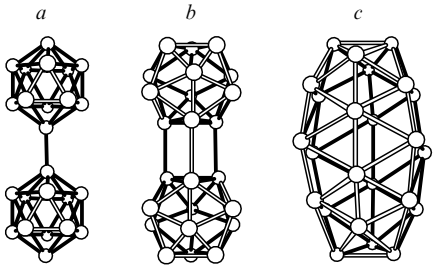


Figure 17. Structural evolution of the B_{24} fragment in the bulk of rhombohedral α-boron quasi-crystal in the course of geometry optimisation.

† According to terminology used in Ref. 57, a 'belt' is a tube segment 'cut' perpendicular to the tube axis, whereas a 'strip' is 'cut' along the tube axis.

Fig. 17 *c*), which can become a 'protoform' of extended nanotubular boron structures.

It was emphasised [43, 132–134] that the structure and properties of proposed nanostructural forms of elemental boron (including a nanotubular form of boron) can differ fundamentally in the presence of impurities of other elements (*e.g.*, carbon, nitrogen, silicon, *etc.*). However, neither detailed studies along this line nor calculations of the electronic structure of the nanotubular form of boron have been carried out so far.

V. Theoretical models of the growth and morphology of nanotubes

One of the fundamental challenges of theoretical investigations is to describe the nature, the kinetics of nucleation and growth, and the morphology of nanotubular structures on the microscopic level.

Thermodynamic aspects of the formation of tubular and spheroidal carbon structures have been discussed.[8, 11, 14] It was emphasised [135, 136] that a symmetry axis determining the direction of the structure growth is required in the reaction zone in order to form tubulenes. In the synthesis of cylindrical structures, such a direction can be specified, *e.g.*, by a beam of accelerated carbon ions [135, 136] or catalysts.[8]

The most widely used method for the NT synthesis is their growth in an electric arc discharge apparatus between graphite electrodes in the presence of various catalysts. It is not possible, in the present state-of-the-art in the field of NT synthesis, to control their size and chirality exactly. Along with NT (or NT bundles whose diameters vary over a wide range), the end product contains fullerenes, other nanoparticles, and soot.[8, 11, 14, 135–138]

The nature and mechanism of NT growth became the subject of discussion in the first studies in which the preparation of NT was reported.[8] Fullerene hemispheres were considered to be precursors,[18, 19, 139, 140] and the growth of tube walls was explained by successive addition of C_2 dimers to the carbon atoms at the hemisphere circumference.

Yet another type of mechanism of SNT growth involving cyclic structures as precursors was proposed.[141] These structures were found in the studies of laser ablation of graphite.[142–144] The most typical structures of C_n species ($10 \leqslant n \leqslant 40$) are planar cyclic structures,[143–145] whereas spheroidal structures are formed at $n > 40$. Two mechanisms of growth of the structures built of carbon rings were suggested,[141] *viz.*, the formation of either a fullerene or an NT. According to the model proposed by Kiang and Goddard,[141] tubular structures are formed due to the presence of catalysts that activate the process.[138]

The model of NT growth from a nucleus (a carbon ring) is illustrated in Fig. 18. In the first stage, a planar ring is distorted in arc plasma in the presence of a catalyst (*e.g.*, cobalt carbide, Co_mC_n) to adopt a *cis*- or a *trans*-form analogously to crystalline carbyne rings.[146] The *cis*-form of the ring can act as a precursor in the synthesis of achiral NT by addition of C_2 dimers. The *trans*-form of the carbon ring may give rise to a larger number of cylindrical structures. The formation of the NT geometry occurs without involving the catalyst species.[141]

In other models of NT growth, the primary emphasis is placed on the role of the substrate and the catalyst. A phenomenological model of mechanism of SNT growth on diamond-like crystallites was proposed.[147] The (111) type of the surface was considered and it was found that the prerequisite for the beginning of the process is the presence of a nanoscale surface defect, *e.g.*, an atom of another element that 'shades' one of the carbon atoms of the upper monatomic layer. A 'nanoisland' that formed is surrounded along its circumference by carbon atoms that have free bonds oriented normal to the surface and interact with the ions in the vapour phase. The ions that precipitate form a ring, an NT 'root' capable of further independent growth. The formation of the first layer according to the model proposed by Chernozatonskii [147] is depicted schematically in Fig. 19 taking a (6, 0)-NT as an example.

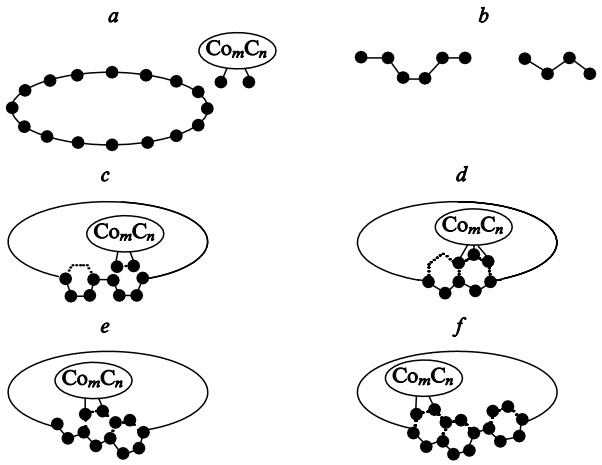


Figure 18. A model of the formation of seeds of nanotubular structures based on cyclic structures: (*a*) initial planar ring; (*b*) local deformation involving the planar ring with the formation of *cis*- and *trans*-forms; (*c*) nucleation of an achiral nanotube based on the *cis*-form; (*d*) nucleation of an achiral nanotube based on the *trans*-form; and (*e*), (*f*) nucleation of chiral nanotubes based on the *trans*-form.

The above-mentioned model [147] is versatile and provides a qualitative explanation for the NT growth under any conditions of their synthesis. An important point is that the size of the nucleus (a surface defect) or that of metal particles (catalysts) should be smaller than the characteristic diameter of the SNT. Then, taking into account that each preceding carbon atom interacts with the 'surface' states of the nanostructure to form its own 'free' bond and becomes an active adsorption centre for the succeeding atom, the process can be interpreted simply.[148]

In the case of metal particles whose size is larger than the characteristic SNT diameter, a carbon (carbide) layer is formed on the surface in the first stage of precipitation, which is then followed by growth of the SNT nuclei (roots). For several metals (*e.g.*, lanthanides) it was found [8, 149, 150] that, depending on the surface morphology, SNT can grow in the form of compact bundles radiating from the nucleus. In this case it is assumed that nanoscale inhomogeneities (protrusions) of the surface of metal grains play the role of 'active nuclei' in the formation of SNT roots.

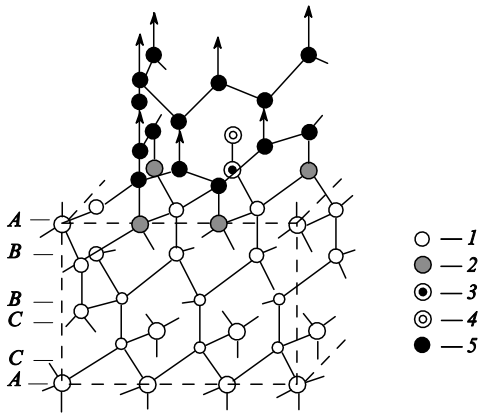


Figure 19. A scheme of the formation of the (6, 0)-NT on the diamond (111) surface. The substrate atoms (*1*), the tube 'root' atoms (*2*) surrounding the surface atom (*3*) 'shaded' by a univalent ion (*4*), and the atoms of tubulene walls (*5*) are shown. The surface (*A*) and near-surface (*B*), (*C*) atomic layers are shown.

A microscopic model of growth of carbon NT on the surface of a metal catalyst was developed.[151] The process on a planar metal surface covered with a hexagonal network of carbon atoms formed upon primary precipitation was considered. Special emphasis was placed on the energy effects upon the rearrangement of the initial layer geometry in the region of curving the elementary polygons that form the SNT base (Fig. 20). It was shown that such a rearrangement results in the formation of pentagons and heptagons. The carbon atoms that precipitated successively on the metal carbide surface migrate toward the SNT base to form 'belts' of hexagons constituting the SNT stem. This provides the possibility for the tube wall surrounding the protrusion on the substrate surface to grow. The model [151] makes it also possible to explain why multilayered NT do not grow.

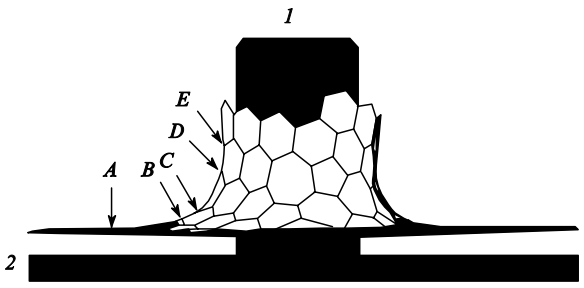


Figure 20. A scheme of growth of single-layered carbon nanotube on a protrusion (*1*) of a surface layer (*2*) of a metal catalyst.
(*A*)–(*E*) are characteristic positions of carbon atoms migrating from the SNT base toward its stem (according to the model by Maiti *et al.*[151]).

Starting from the first study by Iijima,[9] the MNT were considered as a system of ideal coaxial cylinders formed by rolled graphitic sheets. The conditions of the MNT growth depending on the substrate (diamond) structure were considered.[147] It was argued that the presence of the (111) crystallite terraces is a prerequisite for the MNT growth. In this case, 'nucleation ring seeds' consisting of the atoms separated from one another by a distance of several Angström can be distinguished. It has been pointed out that the MNT growth can give rise to intercylindrical interactions and narrowing of the walls of individual NT. As a result, the MNT can be 'shrunk' into cones,[152] thus forming a peculiar kind of 'graphite caps' that close the protrusions of diamond crystallites.

Mention may be made of yet another structural model of a 'quasi-tubular' form of carbon. The conditions under which 'hangars' (multilayer 'arches' of graphene sheets 'resting' on the substrate surface) are formed have been discussed.[147] There are open 'hangars' and those closed at the ends with truncated spheroidal structures.

A growth model of conical multilayered tubular structures was proposed [153] and the possibility of the formation of a helical MNT structure was considered.[154, 155] Successive stages of the growth of helical MNT are shown in Fig. 21. The NT nucleus was assumed to consist of a fullerene hemisphere formed at the substrate surface. Depending on the type of the hemisphere cross section, the 'primary' tube stem can grow in different ways. Ideally, this is a right circular cylinder;[153] however, if the tube base contains pentagons (a 'zigzag' C_{60} cross section), the NT walls can be tilted with respect to the normal to the surface. The first tube type and the corresponding energy of interaction between the pair of graphitic sheets clearly defines the nucleation template (achiral or chiral) of the graphite layer of the next tube walls. The structure of the third sheet (the outer one with respect to the first and second sheets) is not unambiguously defined. This allows mutual reorientations of the system of coaxial tubes (*e.g.*, rotations about a common axis). Effects of NT sliding over one another in MNT have been discussed.[8]

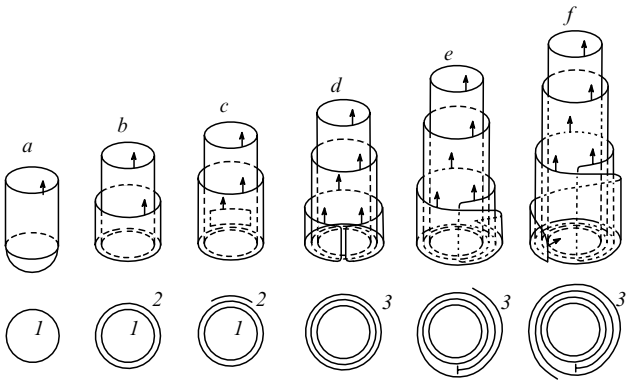


Figure 21. The major stages of growth of helical NT (*a*)–(*f*).[153]
(*1*)–(*3*) graphitic layers in the cross sections of corresponding structures; the edges of dislocations are shown. Arrows indicate the direction of MNT growth.

The increase in the number of graphitic sheets (see Fig. 21) can lead to the formation of lateral dislocations that are considered as energy stabiliser of the system.[153] As a result, the MNT structure is transformed into a helical one and the MNT grows by building up a helix rather than by nucleating the next graphitic sheet. It is of importance that a pair of lateral dislocations of opposite signs should be present in each helical nanotube.

The presence of dislocations will lead to some increase in the tube volume. The MNT growth is terminated when dislocations become oriented parallel to the tube axis.[153]

The authors of the above-mentioned models of MNT growth used qualitative ideas of a specific type of interatomic interactions in the systems in question. Kwon *et al.*[156] studied growth conditions, morphology, and stability of achiral double-layered (5, 5)@(10, 10)- and (9, 0)@(18, 0)-tubulenes consisting of coaxial cylinders with respectively 'arm-chair' and 'zigzag' edges by performing rigorous *ab initio* calculations in the framework of the electron density functional formalism (a cluster model with geometry optimisation according to the DMol version).

During the NT growth process, adatoms can either build up the open end of either tube or connect these ends to become bridging atoms (see respectively configurations *1* and *2*, *3* in Fig. 22). For each of the configurations considered, *ab initio* calculations of energy parameters and electronic structure were carried out. The tube growth was analysed with an increment of 10 extra atoms arranged as described above. Relaxation effects were taken into account by the MD method.

Let us illustrate the results of calculations[156] taking a double-layered (5, 5)@(10, 10)-MNT as an example. Placing extra carbon atoms exactly on the tube edges leads to the formation of a system of 'dangling' bonds. However, in this case the cohesive energies of MNT remain virtually unchanged. For bridging atoms, the

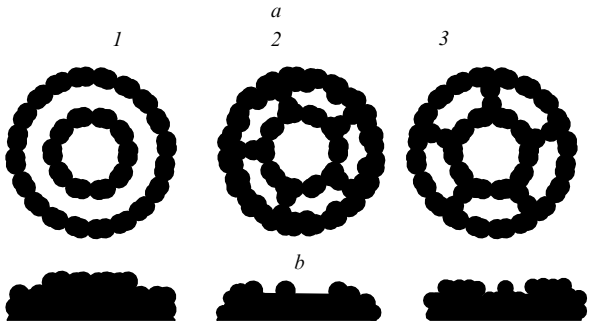


Figure 22. Cross (*a*) and longitudinal (*b*) section of possible growth structures (*1*)–(*3*) of a two-layer (5, 5)@(10, 10)-NT.[156]

situation is markedly different. For a fully optimised structure, the energy gain per each extra atom is rather large ($\Delta E \simeq 0.42$ eV), which confirms the assumption [158] of stabilising contribution of 'lip-lip' interactions between the walls of neighbouring tubes to the total energy of the system. The stabilising effect of bridging atoms depends on their distance from the tube interior and on the type of the polygons formed by these bridging atoms and the atoms of tube walls in the NT cross section. Thus, the configuration *3* in Fig. 22 is unstable ($\Delta E \simeq -3.52$ eV). Analogous conclusions can be drawn from the analysis of the (9, 0)@(18, 0)-MNT. The optimum NT morphology is determined by a combination of the above-mentioned factors.

Ab initio studies of MNT growth and termination depending on the number of extra atoms have also been carried out.[156] The main parameter used in the case of a growing cylindrical MNT was the degree of the edge coverage

$$\varepsilon = \frac{N}{N_a},$$

where N is the total number of carbon atoms on the tube edge and N_a is the number of added (extra) atoms. Then the energy parameter was calculated as a function of ε

$$E_c = \frac{E_{tot}(C_N) - NE_{tot}(C_\infty)}{N_a},$$

where $E_{tot}(C_N)$ is the total energy of the truncated NT of a given length and $E_{tot}(C_\infty)$ is the total energy of an infinite tube.‡ It was assumed that NT growth is favoured to the greatest extent at a minimum E_c value that can be achieved at a certain concentration and for particular configurations of adatoms on the tube edge when the 'growing' tube has a minimum energy as compared to the 'end reaction product', a perfect infinite MNT.

The results of calculations for a (5, 5)@(10, 10)-NT are shown in Fig. 23. Stabilisation of the structure is at $e = 2/3$. The 'lip-lip' interactions play an important role in the structure stabilisation. Stable structures of MNT growth contain carbon hexagons and pentagons, but no squares or triangles. In the range $0 < \varepsilon \leqslant 2$, the initial tube growth is simulated. The interval $2 < \varepsilon \leqslant 4.5$ corresponds to an 'intense edge coverage' of the tubulene. Changes in the relative energies of dome closure, which terminates the process of nanotube growth, are also shown. The simplest types of the domes for closing the inner and outer tubes of the (5, 5)@(10, 10)-NT are hemispheres of the C_{60} and C_{240} fullerenes, respectively. To form closed noninteracting domes, the degree of the edge coverage should lie in the range $8/3 < \varepsilon < 14/3$.

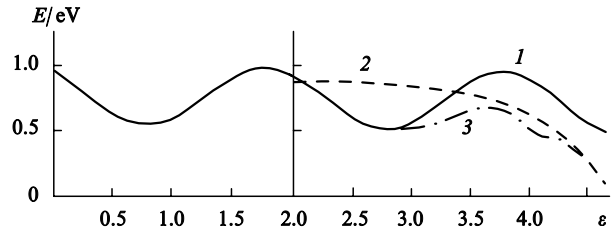


Figure 23. Dependence of the energy (E) of edge groups of the (5, 5)@(10, 10)-NT on the number of adatoms ε (see text). The interval $0 < \varepsilon \leqslant 2$ corresponds to the MNT growth; curves (*1*)–(*3*) in the region $2 < \varepsilon \leqslant 4.6$ describe how E changes for continuous NT growth (*1*) and for the dome closure of the nanotube without (*2*) and with (*3*) account of 'lip-lip' interactions.[156]

The mechanism of double-layered NT growth and conditions of its termination [156] can be extended to MNT with any number of layers. However, problems can arise in the case of odd-walled MNT. It is much more difficult to determine optimum conditions of the saturation of 'dangling bonds' in this case. Probably, MNT with an odd number of layers are less stable. This is indirectly confirmed by larger abundance of MNT with an even number of layers.[158] At the same time, the proposed growth mechanism can be corrected to a certain extent for the presence of 'passivating' elements as impurities ('covalent spot welds') capable of saturating one or several free ('dangling') bonds of the carbon atoms of outer cylinders.

‡ An idealised model of a quasi-1*D* structure is an infinite tube.

VI. Nanotube crystals

Nanotube crystals (NTC) are regular 3*D* structures formed by individual NT.

To date, theoretical models of crystalline nanotubular forms of matter and predictions of their characteristics have been reported only for certain possible crystalline forms of nanotubular carbon. It was suggested that NTC be considered as a new phase of crystalline carbon with quasi-one-dimensional, strongly anisotropic properties.

Progress in the synthesis of single-layered NT and, in particular, the possibility of producing NT of most plausible diameters [6, 8] under specified conditions of plasmochemical process provides an experimental basis for performing theoretical studies. Production of compact nanotubular associates, *e.g.*, NT bundles and ropes, as well as nanotube films with regular arrangement of individual cylinders has been reported.[6, 8, 159–169]

Let us consider the main lines of theoretical investigations of nanotube crystals.

1. Intertubular interactions in nanotube crystals

In the studies of NT packed into regular 3*D* structures, the problem arises of establishing the form of their packing and the nature of interaction between individual NT, and of determining the energy effect of this process. It is assumed [166, 167] that the intertubular bonding is due to the van der Waals interactions (as is the case, *e.g.*, for fullerites [8]).

Optimum ways of packing individual NT into a periodic 3*D* structure were studied.[168] Nanotube crystals formed by (6, 6)-nanotubulenes with parallel cylindrical axes were calculated. Depending on the type of mutual arrangement of individual NT in the nanotube crystal, a tetragonal and a hexagonal unit cell was investigated. In the latter case, calculations were performed for two types of packing of single-layered NT, which correspond to the hypothetical graphite *AAA*... stacking and to the conventional graphite *ABAB*... stacking.

It was found that the system in which carbon atoms of neighbouring tubes are packed similarly to graphite *ABAB*... stacks is the most stable (Fig. 24). In addition, the 'intertubular'

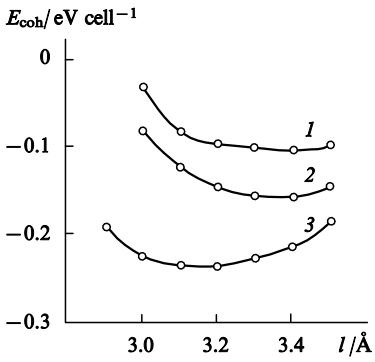


Figure 24. Dependence of the cohesive energy of an NTC formed by (6, 0)-NT on the distance (l) between individual NT for tetragonal (*1*) and hexagonal (*2*), (*3*) unit cells.
Type of the NT packing in hexagonal unit cells: (*AAA*...) (*2*), and (*ABAB*...) (*3*).

cohesive energy E_{coh} in NTC (9.76 meV atom^{-1}) is lower than the interlayer energy in graphite (20 meV atom^{-1})[170] and comparable with the energies of intercluster interactions in condensed fullerenes ($\sim$ 10 meV atom^{-1}). It can be assumed that the conditions of the formation of 3*D* NTC from tubes of different diameters control the degree of close packing of individual NT and the possibility of the *AB* type of packing of the carbon atoms in neighbouring tubes. Any violation of the optimum combination of these factors will lead to destruction of crystal structure and to orientational disorder in the NT arrangement.

The energy band structure of a hexagonal carbon NTC is characteristic of a mixed $1D-3D$ electronic system.[168] The main dispersive effects are due to 'intratubular' interactions; at the same time, intertubular interactions also make a noticeable contribution. The NTC analysed possess a metallic type of conductivity, which means that packing of individual (6, 6)-NT into a crystal does not change the nature of their conductivity.

2. Radial deformations of nanotubulenes in crystals

Charlier *et al.*[168] considered an NTC in which the shape of NT constituting the crystal was assumed to be preset and unchanged upon packing into the 3*D* structure. The problem of possible deformations of SNT in the interaction was posed.[8, 166, 167]

The original concepts of the effect of the interaction between two NT on their cross section geometry were developed by Ruoff *et al.*[166] who calculated structural deformations for a pair of nanotubes using a many-body interaction model. It was established that, first, the walls of neighbouring NT become 'flattened' so that the respective regions of NT reproduce the geometry of planar graphite sheets (which corresponds to a maximum interaction energy) and, second, the intertubular volume is decreased (Fig. 25). It was also pointed out [166] that the degree of deformation depends strongly on the NT diameter and increases as the diameter increases.

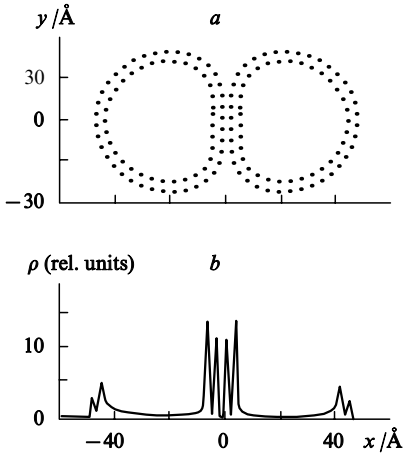


Figure 25. Radial deformations of a pair of contacting NT upon their interaction (*a*) and the charge density ρ distribution (*b*).

The above-mentioned peculiarities of deformation of two individual cylinders upon their packing into a 3*D* structure are clearly illustrated in Fig. 26. The principles of calculations of structural distortions for a pair of contacting cylinders[166] were extended to 3*D* NTC.[167] In Fig. 26, one can clearly see the formation of a 'honeycomb' structure of the NTC cross section with gradual transformation of the cross sections of cylindrical NT into those of hexagonal prisms as the tube diameter increases. In the framework of the model used,[167] the 'flattening' effects of NT walls are detected starting from $d \simeq 15$ Å.

These structural deformations will play an important role in the formation of cohesive and elastic properties of NTC. In the general case, one can expect that the increase in the NT diameter

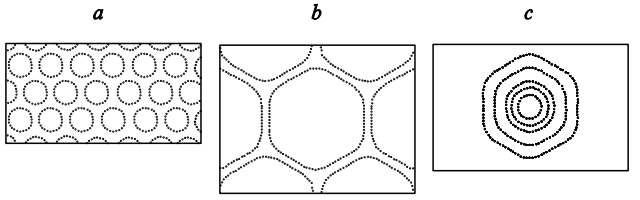


Figure 26. NT deformations in the NTC as a function of tubulene diameter; (*a*) $d = 10$ Å; (*b*) $d = 40$ Å; and (*c*) hexagonal distortions of a nanotube cross section in the crystal with an increase in the NT diameter (for an NT with $d = 10, 15, 20, 30$, and 40 Å). The points correspond to the carbon atoms in the NT cross section.

will be accompanied by weakening of interparticle interactions (in the *XY* plane of the NTC) and reduction of its 2*D* cohesive characteristics. According to calculations,[167] the dependence of the cohesive energy and the modulus of elasticity on the NT diameter is noticeably nonmonotonic (Fig. 27). The formation of a 'honeycomb' structure imparts an anomalous hardness to the NTC that is maintained upon further increase in the diameter (starting from $d \simeq 25$ Å) of NT constituting the crystal. It is suggested that NTC be divided arbitrarily into two groups with 'small' (or 'large') diameters of NT constituting the crystal, possessing respectively a nonmonotonic and a monotonic dependence of the cohesive energy on the NT diameter. Presumably, these groups of NTC will have substantially different physicochemical properties and will respond differently to the effects of doping (*e.g.*, upon introduction of alkali metal ions into intertubular channels) upon the formation of composites, *etc.*

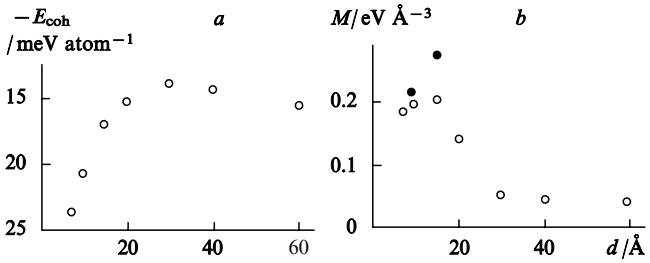


Figure 27. Dependence of the cohesive energy (E_{coh}) (*a*) and the modulus of elasticity (*M*) (*b*) for a nanotube crystal on the diameter (*d*) of nanotubes constituting the NTC. Filled circles correspond to analytical extrapolation of the results of calculations of NTC consisting of nanotubes of small diameter.

3. Hetero-junctions in nanotube crystals

In the formation of 3*D* structures of regularly packed NT it may happen that the geometric and electronic parameters of a pair of neighbouring NT are different or an NTC contains the domains consisting of different NT. It is obvious that in this case one can suggest the existence of 'interphase domains' (or 'interface domains') between nanotube 'polycrystals'. Chico *et al.*[70] considered hetero-junctions in pairs of (12, 0)/(6, 6)- and (9, 0)/(6, 3)-NT and possible differences in electronic properties between the 'interphase domain' and the NT constituents using Green's functions formalism. This study can be considered as the first attempt to describe the above-mentioned systems by semiempirical quantum-chemical methods.

The development of the ideas of condensed regular nanotubular forms of matter as 3*D* periodic structures, *viz.*, nanotube crystals, makes it possible to consider these solids taking into account all factors determining the 'composition–structure–properties' interrelations inherent in all 'conventional' solids.

Assuming that isolated nanotubes whose properties can be varied over a wide range can be considered as 'structural elements'

of NTC, one can accept the idea of a defect (impurity, vacancy) structure of NTC and consider the order–disorder problem therein. Such an approach makes it possible to consider NTC in the context of general problems of the description of specific properties of crystals (including electronic ones) and to pose the problems of surface states of NTC, interfaces between nanotube polycrystals, *etc*.

The above-mentioned lines of the development of the ideas concerning fundamental properties of NTC are still in a primitive state even for carbon NTC. One can expect that they will be useful for the development of the problems of quantum materials science and their application to NTC forms of other substances including those considered in this review.

VII. Conclusion

The discovery of the nanotubular form of matter was one of the major achievements of physical chemistry in the last decade. Unique properties of nanotubulenes offer extremely attractive prospects of their use in technology and are of considerable interest for fundamental research.

Only the principal results of the studies of electronic structure of NT by methods of solid state quantum chemistry have been covered in this review. The most considerable progress has been achieved in the studies of single-layered isolated nanotubes and prediction of their properties.

Recent studies on the synthesis of NT and nanotubular materials [171–174] are intimately associated with the development of theoretical models. One of the most important theoretical problems is to describe the 'life cycle' of tubulenes (nucleation–growth–disintegration). Currently, considerable interest is demonstrated in 'intermediate' nanoscale forms (barrellenes,[175–177] onions,[178] calabashes,[179] and other nanoscale structures and mesostructures [180, 181]) which can act as intermediates in the formation or disintegration of NT.[182]

Topical are investigations of various nanotubular structures (tori,[183–185] cones,[186] nanotubes with negative Gaussian curvature,[187] quasi-2*D* NT associates, and nanotubular layers and films [188–191]), nanotubular superstructures,[191–194] and 'mixed' nanoscale forms and composites (*e.g.*, NT-fullerene,[195] amorphous nanotubular carbon [196]) which can possess unusual properties.

The theory of adsorptive, capillary, electromagnetic, catalytic, mechanical, and other properties of NT that are of interest for researchers in the field of materials science is in the early stage.

The problem of whether the nanotubular form of matter is a universal form for the whole known diversity of inorganic substances or are there certain physical or chemical criteria clearly reducing the number of potential objects whose nanotubular forms can be obtained under certain (which?) conditions, is a basic problem which remains open so far.

The solution of the above-mentioned problems is one of the priorities in the quantum chemistry of nanotubulenes. It provides a basis for the development of the tubulene materials science, thus favouring their effective use in nanoscale electronics, in instruments and chemical engineering, and in other areas.

References

1. H W Kroto, A W Allaf, S P Balm *Chem. Rev.* **91** 1213 (1991)
2. V I Sokolov, I V Stankevich *Usp. Khim.* **62** 455 (1993) [*Russ. Chem. Rev.* **62** 419 (1993)]
3. R A Andrievskii *Usp. Khim.* **63** 431 (1994) [*Russ. Chem. Rev.* **63** 411 (1994)]
4. T W Ebbesen *Ann. Rev. Mater. Sci.* **24** 235 (1994)
5. Y Tenne *Adv. Mater.* **7** 965 (1995)
6. T W Ebbesen *Phys. Today* **273** 26 (1996)
7. V M Smirnov *Khimiya Nanostruktur. Sintez, Stroenie, Svoistva* (The Chemistry of Nanostructures. Synthesis, Structure, Properties) (St.-Petersburg: St.-Petersburg State University, 1996)
8. M S Dresselhaus, G Dresselhaus, P C Eklund *Science of Fullerenes and Carbon Nanotubes* (New York: Academic Press, 1996)
9. S Iijima *Nature (London)* **354** 56 (1991)
10. T W Ebbesen, P M Ajayan *Nature (London)* **358** 220 (1992)
11. S Iijima, T Ichihashi *Nature (London)* **363** 603 (1993)
12. S Iijima, P M Ajayan, T Ichihashi *Phys. Rev. B, Condens. Matter* **47** 5485 (1993)
13. S Iijima, P M Ajayan, T Ichihashi *Phys. Rev. Lett.* **69** 3100 (1992)
14. D S Bethune, C H Kiang, M S de Vries, G Gorman, R Savoy, J Vazquez, R Beyers *Nature (London)* **363** 605 (1993)
15. P M Ajayan, J M Lambert, P Bernier, L Barbedette, C Colliex, J M Planeix *Chem. Phys. Lett.* **215** 509 (1993)
16. P Calvert *Nature (London)* **357** 365 (1992)
17. J W Mintmire, B I Dunlap, C T White *Phys. Rev. Lett.* **68** 631 (1992)
18. R Saito, M Fujita, G Dresselhaus, M S Dresselhaus *Phys. Rev. B, Condens. Matter* **46** 1804 (1992)
19. R Saito, M Fujita, G Dresselhaus, M S Dresselhaus *Appl. Phys. Lett.* **60** 2204 (1992)
20. B I Dunlap *Phys. Rev. B, Condens. Matter* **46** 1933 (1992)
21. N Hamada, S Sawada, A Oshiyama *Phys. Rev. Lett.* **68** 1579 (1992)
22. M S Dresselhaus, G Dresselhaus, R Saito *Solid State Commun.* **84** 201 (1992)
23. M S Dresselhaus, G Dresselhaus, R Saito *Phys. Rev. B, Condens. Matter* **45** 6234 (1992)
24. A Oshiyama, S Saito, N Hamada, Y Miyamoto *J. Phys. Chem. Solids* **53** 1457 (1992)
25. M S Dresselhaus *Phys. World* **9** 18 (1996)
26. M Menon, D Srivastava *Phys. Rev. Lett.* **79** 4453 (1997)
27. R Saito *Science* **278** 77 (1997)
28. P G Collins, A Zettl, H Bando, A Thess, R E Smalley *Science* **278** 100 (1997)
29. A Lorezoni, H E Roman, F Alasia, R A Broglia *Chem. Phys. Lett.* **276** 237 (1997)
30. E W Wong, P E Sheehan, C M Lieber *Science* **277** 1971 (1997)
31. M S Dresselhaus *Nature (London)* **391** 19 (1998)
32. P Gleize, M C Schouler, P Gadelle, M Caillet *J. Mater. Sci.* **29** 1575 (1994)
33. P Gleize, S Herreyre, P Gadelle, H Mermoux, M C Cheynet, L Abello *J. Mater. Sci. Lett.* **13** 1413 (1994)
34. N G Chopra, R J Luyken, K Cherrey, V H Crespi, M L Cohen, S G Louie, A Zettl *Science* **269** 966 (1995)
35. A Loiseau, F Willaime, N Demoncy, G Hug, H Pracard *Phys. Rev. Lett.* **76** 4737 (1996)
36. A Zettl *Adv. Mater.* **8** 443 (1996)
37. Z Weng-Sieh, K Cherrey, N G Chopra, X Blase, Y Miyamoto, A Rubio, M L Cohen, S G Louie, A Zettl, R Gronsky *Phys. Rev. B, Condens. Matter* **51** 1129 (1995)
38. O Stephan, P M Ajayan, C Colliex, P Redlich, J Lambert, P Bernier, P Lefin *Science* **266** 1683 (1994)
39. Y Feldman, E Wasserman, D J Srolovitz, R Tenne *Science* **267** 222 (1995)
40. M Remskar, Z Skraba, F Cleton, R Sanjines, F Levy *Appl. Phys. Lett.* **69** 351 (1996)
41. H Nakamura, Y Matsui *Adv. Mater.* **7** 871 (1995)
42. H L Frisch, J E Mark *Chem. Mater.* **8** 1735 (1996)
43. I Boustani, A Quandt *Europhys. Lett.* **39** 527 (1997)
44. W K Hsu, J P Hare, M Terrones, H W Kroto, D Walton, P Harris *Nature (London)* **377** 687 (1995)
45. M Freemantle *Chem. Eng. News* **73** 9 (1995)
46. J W Wildler, L C Venema, A Rinzler, R E Smalley, C Dekker *Nature (London)* **391** 59 (1998)
47. T W Odom, J-L Huang, P Kim, C M Lieber *Nature (London)* **391** 62 (1998)
48. J W Mintmire, D H Robertson, C T White *J. Phys. Chem. Solids* **54** 1835 (1993)
49. H Yorikawa, S Muramatsu *Phys. Rev. B, Condens. Matter* **50** 12203 (1994)
50. J W Mintmire, C T White *Synth. Met.* **77** 231 (1996)
51. H Yorikawa, S Muramatsu *Solid State Commun.* **94** 435 (1996)
52. R Saito, G Dresselhaus, M S Dresselhaus *Phys. Rev. B, Condens. Matter* **50** 14698 (1994)
53. H Ajiki, T Ando *J. Phys. Soc. Jpn.* **62** 1255 (1993)
54. H Yorikawa, S Muramatsu *Phys. Rev. B, Condens. Matter* **52** 2723 (1995)

55. H Yorikawa, S Muramatsu *Solid State Commun.* **97** 115 (1996)
56. I V Zaporotskova, A O Litinskii *Vest. Volgogradsk. Gos. Univ.* (1) 145 (1997)
57. I V Zaporotskova, Candidate Thesis in Physicomathematical Sciences, Volgograd State University, Volgograd, 1997
58. M S Dresselhaus, G Dresselhaus *Adv. Phys.* **30** 139 (1981)
59. D Tomanek, M A Schluter *Phys. Rev. Lett.* **67** 2331 (1991)
60. D H Robertson, D W Brenner, J W Mintmire *Phys. Rev. B, Condens. Matter* **45** 12592 (1992)
61. J Tersoff *Phys. Rev. B, Condens. Matter* **37** 6991 (1988)
62. D W Brenner *Phys. Rev. B, Condens. Matter* **42** 9458 (1990)
63. J W Mintmire, C T White *Phys. Rev. B, Condens. Matter* **28** 3283 (1983)
64. J W Mintmire *Phys. Rev. Lett.* **50** 101 (1983)
65. C N R Rao, R Seshadri, A Govindaraj, R Sen *Mater. Sci. Eng.* **R15** 209 (1995)
66. D Östling, D Tomanek, A Rosen *Phys. Rev. B, Condens. Matter* **55** 13980 (1997)
67. J Yi, J Bernholc *Phys. Rev. B, Condens. Matter* **47** 1708 (1993)
68. R Car, M Parrinello *Phys. Rev. Lett.* **55** 2471 (1985)
69. A O Litinskii, N G Lebedev, I V Zaporotskova *Zh. Fiz. Khim.* **69** 189 (1995) [a]
70. L Chico, L X Benedict, S G Louie, M L Cohen *Phys. Rev. B, Solid State* **54** 2600 (1996)
71. R Landauer *Philos. Mag.* **21** 863 (1970)
72. D S Fisher, P A Lee *Phys. Rev. B, Condens. Matter* **23** 6851 (1981)
73. J C Charlier, P Lambin, T W Ebbesen *Phys. Rev. B, Condens. Matter* **54** R8377 (1996)
74. S Seraphin, D Zhou, J Jiao *Acta Microscop.* **3** 45 (1994)
75. M Liu, J M Cowley *Ultramicroscopy* **53** 333 (1994)
76. M Liu, J M Cowley *Carbon* **32** 393 (1994)
77. H Hiura, T W Ebbesen, J Fujita, K Tanigaki, T Takada *Nature (London)* **367** 148 (1994)
78. M S Dresselhaus *Nature (London)* **358** 195 (1992)
79. M S Dresselhaus, G Dresselhaus, R Saito *Carbon* **33** 883 (1995)
80. R Heyd, A Charlier, E McRae *Phys. Rev. B, Condens. Matter* **55** 6820 (1997)
81. Y Miyamoto *Phys. Rev. B, Condens. Matter* **54** R11149 (1996)
82. J Despers, E Daguerre, K Ladfi *Carbon* **33** 87 (1995)
83. N Chopra, L Benedict, V Crespi, M Cohen, S Louie, A Zettl *Nature (London)* **377** 135 (1995)
84. R S Ruoff, D C Lorents *Bull. Am. Phys. Soc.* **40** 173 (1995)
85. C Lieber *Bull. Am. Phys. Soc.* **42** 591 (1997)
86. S Iijima, C Brabec, A Maiti, J Bernholc *J. Chem. Phys.* **104** 2089 (1996)
87. T W Ebbesen, in *Carbon Nanotubes. Preparation and Properties* (Ed. T W Ebbesen) (Boca Raton, FL: CRC Press, 1997) p. 225
88. B I Yakobson, M B Campbell, C J Brabec, J Bernholc *Comput. Mater. Sci.* **8** 341 (1997)
89. J Lu *Phys. Rev. Lett.* **79** 1297 (1997)
90. M R Falko, C H Clary, R M Taylor, V Chi, F P Brooks, S Washburn, R Superfine *Nature (London)* **389** 582 (1997)
91. B I Yakobson, C J Brabec, J Bernholc *Phys. Rev. Lett.* **76** 2511 (1996)
92. G Adams *Science* **256** 1792 (1992)
93. A Lucas, P Lambin, R Smalley *J. Phys. Chem. Solids* **54** 587 (1993)
94. K Akagi, R Tamura, M Tsukada, S Itoh, S Ihara *Phys. Rev. B, Condens. Matter* **53** 2116 (1996)
95. S Ihara, S Itoh, J Kitakami *Phys. Rev. B, Condens. Matter* **48** 5643 (1993)
96. X B Zhang, X F Zhang, D Bernaerts, G van Tendeloo, S Amelinckx, J van Landuyt, V Ivanov, J B Nagy, Ph Lambin, A A Lucas *Europhys. Lett.* **27** 141 (1994)
97. V Ivanov, J B Nagy, Ph Lambin, A Lucas, X B Zhang, X F Zhang, D Bernaerts, G van Tendeloo, S Amelinckx, J van Landuyt *Chem. Phys. Lett.* **223** 329 (1994)
98. S Ichara, S Itoh, J Kitakami *Phys. Rev. B, Condens. Matter* **47** 12908 (1993)
99. B I Dunlap *Phys. Rev. B, Condens. Matter* **49** 5643 (1994)
100. B I Dunlap *Phys. Rev. B, Condens. Matter* **50** 8134 (1994)
101. S Itoh, S Ichara *Phys. Rev. B, Condens. Matter* **48** 8323 (1993)
102. S Itoh, S Ichara *Phys. Rev. B, Condens. Matter* **47** 1703 (1993)
103. K Akagi, R Tamura, M Tsukada, S Ihara, S Itoh *Phys. Rev. Lett.* **74** 2307 (1995)
104. M Fujita *Fullerene Sci. Technol.* **1** 365 (1993)
105. Y Saito, K Hamaguchi, K Hata, K Uchida, Y Tasaka, F Ikazaki, M Yumura, A Kasuya, Y Nishina *Nature (London)* **389** 27 (1997)
106. R Saito, G Dresselhaus, M S Dresselhaus *Phys. Rev. B, Condens. Matter* **53** 2044 (1996)
107. J C Charlier, T W Ebbesen, P Lambin *Phys. Rev. B, Condens. Matter* **53** 11108 (1996)
108. R A Jiski, M S Dresselhaus *Phys. Rev. B, Condens. Matter* **45** 12465 (1992)
109. P M Ajayan, S Iijima *Nature (London)* **361** 333 (1993)
110. E Dujardin, T W Ebbesen, H Hiura, K Tanigaki *Science* **265** 1850 (1994)
111. C Guerret-Plecourt, Y Le Bouar, A Loiseau, H Prasacard *Nature (London)* **372** 761 (1994)
112. P M Ajayan, C Colliex, J M Lambert, P Bernier, L Barbedette, M Tence, O Stephan *Phys. Rev. Lett.* **72** 1722 (1994)
113. K Tanaka, T Sato, T Yamabe, K Okahara, K Uchida, M Yumura, H Niino, S Ohshima, Y Kuriki, K Yase, F Ikazaki *Chem. Phys. Lett.* **223** 65 (1994)
114. P M Ajayan, T W Ebbesen, T Ichihashi, S Iijima, K Tanigaki, H Hiura *Nature (London)* **362** 522 (1993)
115. S Seraphin, D Zhou, J Jiao, J C Withers, R Loutfy *Nature (London)* **362** 503 (1993)
116. S Subramoney, R S Ruoff, D C Lorents, B Chan, R Malhotra, M J Dyer, K Parvin *Carbon* **32** 507 (1994)
117. S C Tsang, Y K Chen, P Harris, M Green *Nature (London)* **372** 159 (1994)
118. S Salomonson, P Oster *Phys. Rev. A, Gen. Phys., Ser. 3* **40** 5559 (1989)
119. Y Miyamoto, A Rubio, X Blase, M L Cohen, S G Louie *Phys. Rev. Lett.* **74** 2992 (1995)
120. J A Wu, M L Wang, R Lu, W H Duan *Int. J. Mod. Phys.* **B12** 1601 (1998)
121. X Blase, L X Benedict, E L Shirley, S G Louie *Phys. Rev. Lett.* **72** 1878 (1994)
122. A Rubio, J L Corkill, M L Cohen *Phys. Rev. B, Condens. Matter.* **49** 5081 (1994)
123. Y Miyamoto, A Rubio, M L Cohen, S G Louie *Phys. Rev. B, Condens. Matter* **50** 4976 (1994)
124. Y Miyamoto, A Rubio, S G Louie, M L Cohen *Phys. Rev. B, Condens. Matter* **50** 18360 (1994)
125. A L Ivanovskii *Usp. Khim.* **66** 511 (1997) [*Russ. Chem. Rev.* **66** 459 (1997)]
126. A L Ivanovskii, G P Shveikin *Kvantovaya Khimiya v Materialovedenii. Bor, Ego Splavy i Soedineniya* (Quantum Chemistry for Materials Technology. Boron, Its Alloys and Compounds) (Ekaterinburg: Izd. 'Ekaterinburg', 1997)
127. H Zhu, D J Klein, W A Seitz, N H March *Inorg. Chem.* **34** 1377 (1995)
128. A Rubio, Y Miyamoto, X Blase, M L Cohen, S G Louie *Phys. Rev. B, Condens. Matter* **53** 4023 (1996)
129. Y Miyamoto, S G Louie, M L Cohen, *Phys. Rev. Lett.* **76** 2121 (1996)
130. I Boustani, *Int. J. Quantum. Chem.* **52** 1081 (1994)
131. I Boustani *Chem. Phys. Lett.* **240** 135 (1995)
132. I Boustani, A Quandt, P Kramer *Europhys. Lett.* **36** 583 (1996)
133. I Boustani, in *Proceedings of the 12th International Symposium on Boron, Borides, Related Compounds (Abstracts of Reports), Vienna, 1996* p. 14
134. I Boustani *Phys. Rev. B, Condens. Matter* **55** 101 (1997)
135. C-H Kiang, W A Goddard III, R Beyers, J R Salem, D S Bethune *J. Chem. Phys.* **98** 6612 (1994)
136. S Seraphin, D Zhou *Appl. Phys. Lett.* **64** 2087 (1994)
137. Y Saito, M Okuda, N Fujimoto, T Yoshikawa, M Tomita, T Hayashi *Jpn. J. Appl. Phys., Part 2* **33** L526 (1994)
138. C-H Kiang, W A Goddord, R Beyers, J R Salem, D S Bethune *J. Phys. Chem. Solids* **57** 35 (1996)
139. R Saito, M Fujita, G Dresselhaus, M S Dresselhaus *Mater. Sci. Eng.* **19B** 185 (1993)
140. M Endo, H W Kroto *J. Phys. Chem.* **96** 6941 (1992)
141. C-H Kiang, W A Goddard *Phys. Rev. Lett.* **76** 2515 (1996)
142. G von Helden, N G Gotts, M T Bowers *Nature (London)* **363** 60 (1993)
143. J Hunter, J Fye, M F Jarrold *Science* **260** 784 (1993)

144. J Hunter, J Fye, E J Roskamp, M F Jarrold *J. Phys. Chem.* **98** 1810 (1994)
145. G von Helden, P R Kemper, N G Gotts, M T Bowers *Science* **259** 1300 (1993)
146. R B Heinman, J Kleiman, N M Salansky *Nature (London)* **306** 164 (1983)
147. L A Chernozatonskii *Khim. Fiz.* **16** 78 (1997) [b]
148. C J Brabec, A Maiti, C Roland, J Bernholc *Chem. Phys. Lett.* **236** 150 (1995)
149. D Zhou, S Seraphin, S Wang *Appl. Phys. Lett.* **65** 1593 (1994)
150. S Subramoney, R S Ruoff, D C Lorents, R Malhotra *Nature (London)* **366** 637 (1993)
151. A Maiti, C J Brabec, J Bernholc *Phys. Rev. B, Condens. Matter* **55** R6097 (1997)
152. M Ge, K Sattler *Chem. Phys. Lett.* **220** 192 (1994)
153. S Amelinckx, D Bernaerts, X B Zhang, G van Tendeloo, J van Landuyt *Science* **267** 1334 (1995)
154. X F Zhang, X B Zhang, G van Tendeloo, S Amelinckx, M Op de Beek, J van Landuyt *J. Cryst. Growth* **130** 368 (1993)
155. X B Zhang, X F Zhang, S Amelinckx, G van Tendeloo, J van Landuyt *Ultramicroscopy* **54** 237 (1994)
156. Y K Kwon, Y H Lee, S G Kim, P Jund, D Tomanek, R E Smalley *Phys. Rev. Lett.* **79** 2065 (1997)
157. B Delley *J. Chem. Phys.* **92** 508 (1990)
158. D Tomanek *NATO ASI, Ser. B* **313** 405 (1996)
159. W A de Heer, M S Basca, A Chatelain, T Gerfin, R Humphrey-Baker, L Forro, D Ugarte *Science* **268** 845 (1995)
160. O Chauvet, L Forro, W Bacsa, D Ugarte, B Doudin, W A Heer *Phys. Rev. B, Condens. Matter* **52** R6963 (1995)
161. J C Charlier, J-P Issi *J. Phys. Chem. Solids* **57** 957 (1996)
162. J E Fisher, H Dai, A Thess, R Lee, N M Hanjani, D L Dehaas, R Smalley *Phys. Rev. B, Condens. Matter* **55** R4921 (1997)
163. H Dai, E Wong, C Lieber *Science* **272** 523 (1996)
164. L Langer, V Bayot, E Grivel, J-P Issi, J P Heremanas, C H Olk, L Stocman, C van Haesendonck, Y Bruynseraede *Phys. Rev. Lett.* **76** 479 (1996)
165. G Baumgartner, M Carrard, L Zuppiroli, M S Basca *Phys. Rev. B, Condens. Matter* **55** 6704 (1997)
166. R S Ruoff, J Tersoff, D C Lorents, S Subramoney, B Chan *Nature (London)* **364** 514 (1993)
167. J Tersoff, R S Ruoff *Phys. Rev. Lett.* **73** 676 (1994)
168. J C Charlier, X Gonze, J P Michenaud *Europhys. Lett.* **29** 43 (1995)
169. J C Charlier, X Gonze, J P Michenaud *Carbon* **32** 289 (1994)
170. P M Ajayan, S Iijima *Nature (London)* **358** 23 (1992)
171. Yu E Lozovik, A M Popov *Usp. Fiz. Nauk* **167** 751 (1997) [c]
172. P M Ajayan, T W Ebbesen *Rep. Prog. Phys.* **60** 1025 (1997)
173. A Nikolic, V Radomolivic, M Simicic, D Koruga *Adv. Mater. Process.* **282** 83 (1998)
174. A V Eletskii *Usp. Fiz. Nauk* **167** 945 (1997) [c]
175. E G Gal'pern, I V Stankevich, L A Chernozatonskii, A L Chistyakov *Pis'ma Zh. Eksp. Teor. Fiz.* **56** 483 (1992)
176. Z Ya Korsakovskaya, L A Chernozatonskii, E A Fedorov *Pis'ma Zh. Eksp. Teor. Fiz.* **56** 26 (1992)
177. L A Chernozatonskii *Phys. Lett.* **A166** 55 (1992)
178. E D Obraztsova, M Fujii, S Hyashi, V L Kuznetsov, Y V Butenko *Carbon* **36** 821 (1998)
179. Z L Wang, J S Yin *Chem. Phys. Lett.* **289** 189 (1998)
180. P J F Harris *Int. Mater. Rev.* **42** 206 (1998)
181. P Schraff *Carbon* **36** 481 (1998)
182. B Wei, J Zhang, J Liang, D Wu *Carbon* **36** 997 (1998)
183. L A Chernozatonskii *Phys. Lett.* **A170** 37 (1992)
184. E G Gal'pern, I V Stankevich, L A Chernozatonskii, A L Chistyakov *Fullerene Sci. Technol.* **2** 1 (1994)
185. V Meunier, Ph Lambin, A A Lucas *Phys. Rev. B, Solid State* **57** 14 886 (1998)
186. J Han, R Jaffe *J. Chem. Phys.* **108** 2817 (1998)
187. H Terrones, M Terrones *Carbon* **36** 725 (1998)
188. L A Chernozatonskii *Phys. Lett.* **A172** 173 (1992)
189. L A Chernozatonskii, E F Kukovitskii, A L Musatov, A B Ormont, S G L'vov *Carbon* **36** 713 (1998)
190. J Lefebvre, R Antonov, A T Johnson *J. Appl. Phys.* **A67** 71 (1998)
191. B An, S Fukuyama, K Yokogawa, M Yoshimura *Jpn. J. Appl. Phys.* **37** 3809 (1998)
192. E G Gal'pern, I V Stankevich *Mol. Mater* **C8** 169 (1996)
193. L A Chernozatonskii *Mol. Mater* **C7** 41 (1996)
194. E G Gal'pern, I V Stankevich, A L Chistyakov, L A Chernozatonskii *Fullerene Sci. Technol.* **6** 499 (1998)
195. T Kukumaki, T Hayashi, K Miyazawa, H Ichinose, K Ito, Y Ishida *Mater. Trans. JIM* **39** 574 (1998)
196. G van Tendeloo, D Bernaerts, S Amelinckx *Carbon* **36** 487 (1998)
197. A L Ivanovskii *Kvantovaya Khimiya v Materialovedenii. Nanotubulyarnye Formy Veshchestva* (Quantum Chemistry in Materials Technology. Nanotubular Forms of Substance) (Ekaterinburg: Ural Brunch Russian Academy of Sciences, 1999)

[a] — *Russ. J. Phys. Chem. (Engl. Transl.)*
[b] — *J. Chem. Phys. (Engl. Transl.)*
[c] — *Physics-Uspekhi (Engl. Transl.)*